

Non-perturbative effects on the q_T spectrum of the Z boson

Valerio Bertone

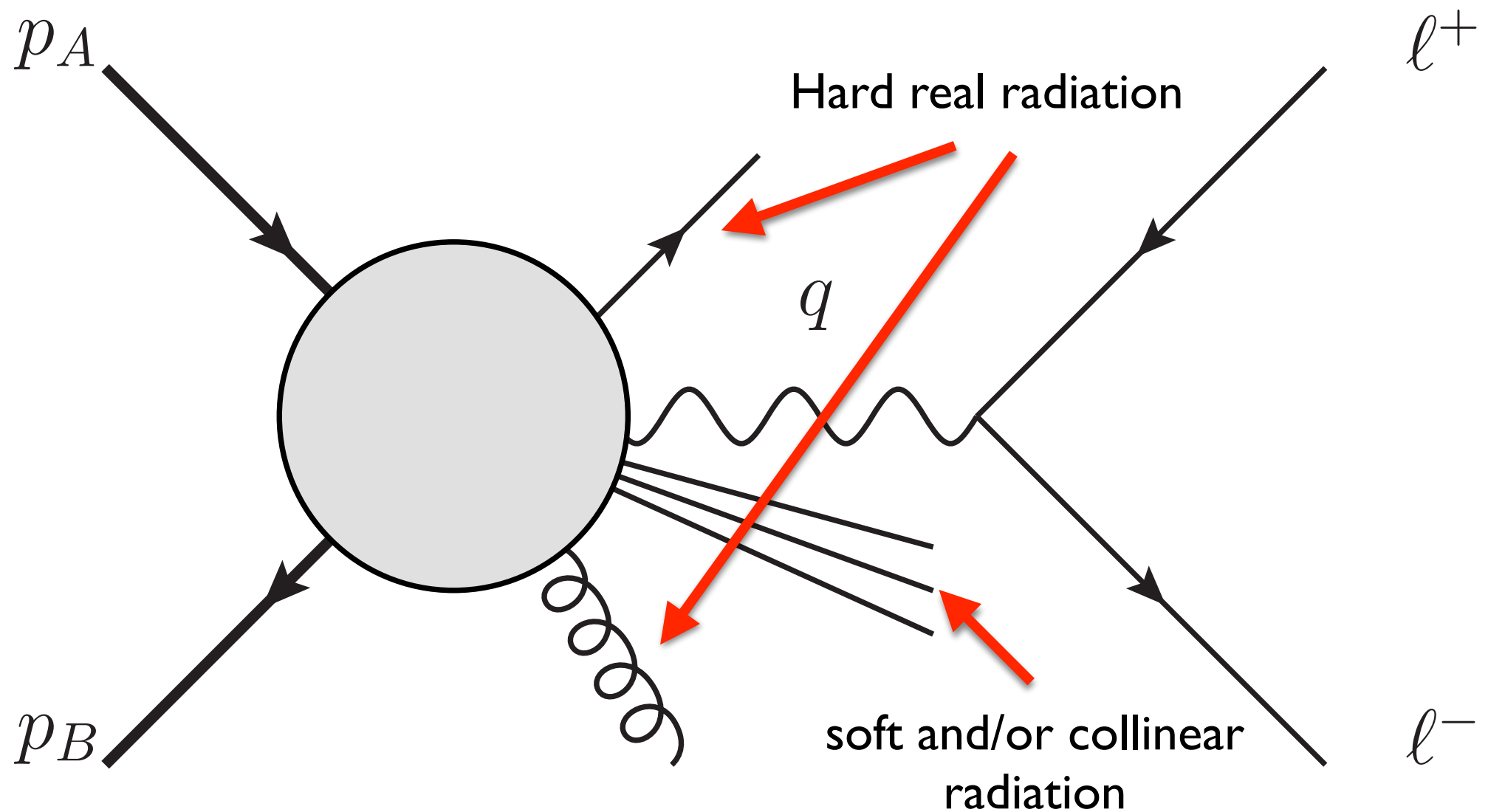
IRFU, CEA, Université Paris-Saclay



June 30, 2025, GDR workshop on W mass, Orsay

Drell-Yan production

- ▀ Inclusive production of a lepton pair in pp collisions:



- ▀ Relevant scales:

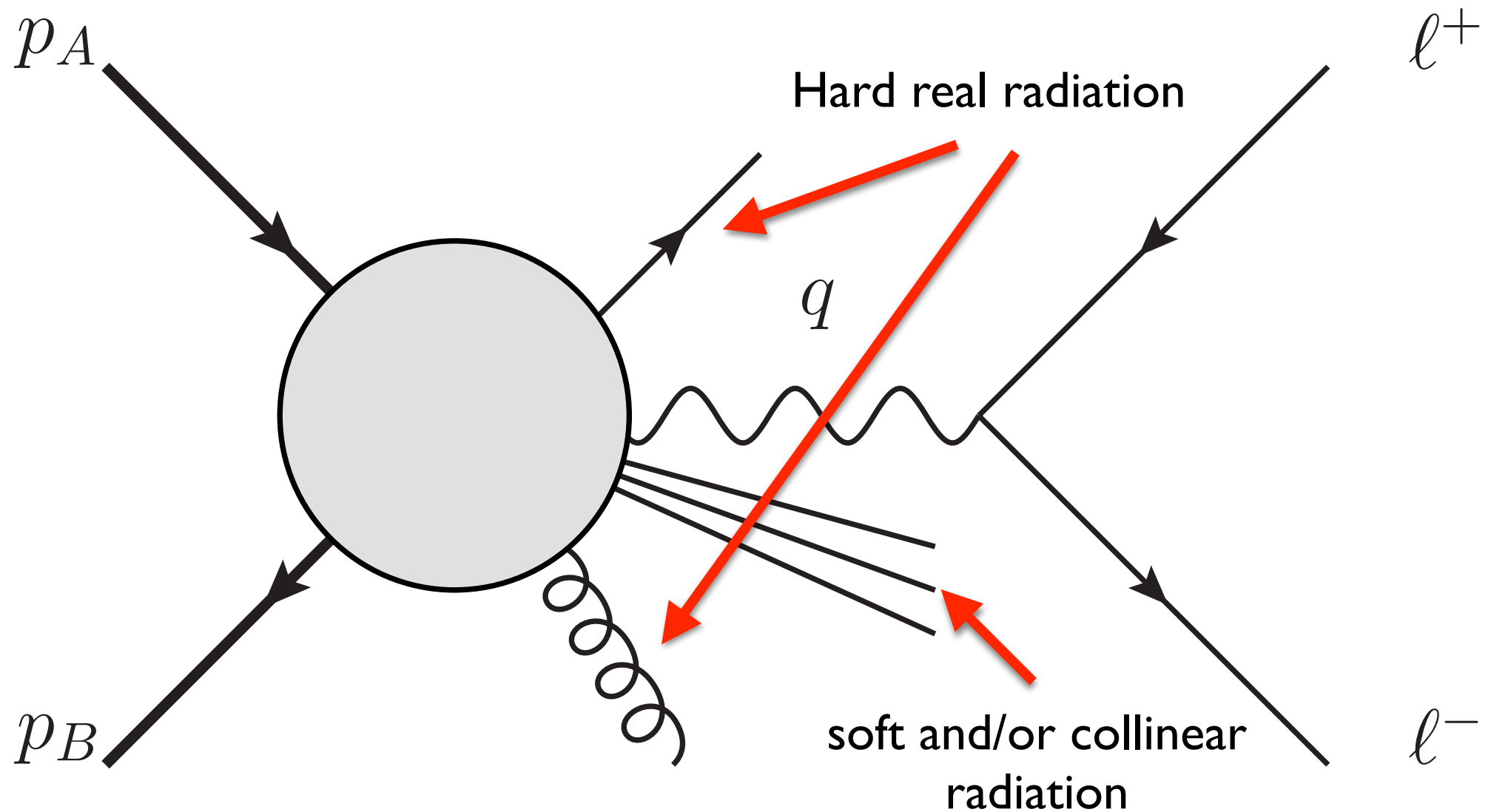
$$Q = \sqrt{q^2},$$

$$q_T,$$

$$Q \gg \Lambda_{\text{QCD}}$$

Drell-Yan production

- ▀ Inclusive production of a lepton pair in pp collisions:

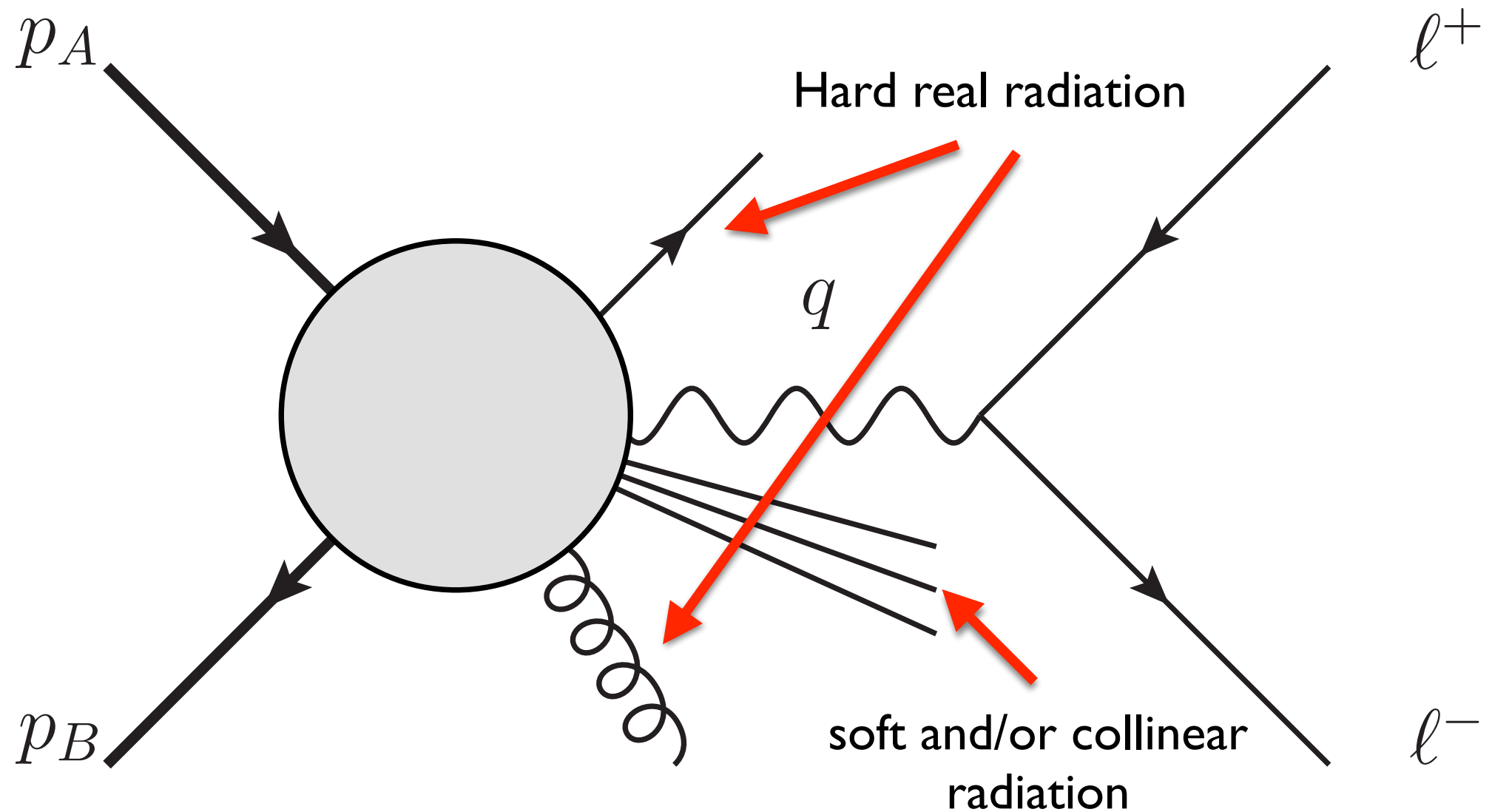


- ▀ Regime 1: $q_T \simeq Q$

- ▀ There must be real **hard radiation** to generate large q_T .
- ▀ **Insensitivity** to intrinsic transverse momentum of partons ($k_T \simeq \Lambda_{\text{QCD}}$).
- ▀ Soft radiation under control, collinear radiation resummed via DGLAP.

Drell-Yan production

- ▀ Inclusive production of a lepton pair in pp collisions:



- ▀ Regime 2: $q_T \ll Q$

- ▀ Hard radiation inhibited, only **soft and/or collinear radiation** allowed.
- ▀ Sensitivity to parton **intrinsic transverse momentum** (when $q_T \approx \Lambda_{\text{QCD}}$).
- ▀ Soft and collinear radiation resummed via TMD evolution and matching⁴

Factorisations

- 🍎 The two regimes obey two different factorisation theorems:
 - 🍎 for $q_T \simeq Q$ **collinear factorisation** at *fixed perturbative order* is appropriate:
$$\left(\frac{d\sigma}{dq_T} \right)_{\text{f.o.}} = \int_{x_1}^1 \frac{dy_1}{y_1} \int_{x_2}^1 \frac{dy_2}{y_2} f_1(y_1, \mu) f_2(y_2, \mu) \frac{d\hat{\sigma}}{dq_T} \left(\frac{x_1}{y_1}, \frac{x_2}{y_2}, \mu, Q \right)$$
 - 🍎 for $q_T \ll Q$ **transverse-momentum-dependent (TMD) factorisation** at *fixed logarithmic order* is appropriate:
$$\begin{aligned} \left(\frac{d\sigma}{dq_T} \right)_{\text{res.}} &= \sigma_0 H(Q, \mu) \int d^2 k_{T1} d^2 k_{T2} F_1(x_1, k_{T1}, \mu, \zeta_1) F_2(x_2, k_{T2}, \mu, \zeta_2) \delta^{(2)}(q_T - k_{T1} - k_{T2}) \\ &= \sigma_0 H(Q, \mu) \int_0^\infty db_T b_T J_0(b_T q_T) F_1(x_1, b_T, \mu, \zeta_1) F_2(x_2, b_T, \mu, \zeta_2) \end{aligned}$$
- 🍎 Collinear and TMD factorisations can be **matched** to produce accurate results over the full q_T spectrum.

Resummation formalisms

- 🍎 Different formulations of the q_T spectrum valid for $q_T \ll Q$ and $q_T \gg \Lambda_{\text{QCD}}$:

$$\left(\frac{d\sigma}{dq_T}\right)_{\text{res.}} \propto \begin{cases} e^{2S} [f_1 \otimes \mathcal{H} \otimes f_2] & : q_T \text{ resum.} \\ H \times B_1 \times B_2 \times S & : \text{SCET} \\ H \times F_1 \times F_2 & : \text{TMD} \end{cases} + \mathcal{O}\left[\left(\frac{\Lambda_{\text{QCD}}}{q_T}\right)^n, \left(\frac{q_T}{Q}\right)^m\right]$$

- 🍎 All of them **resum** large $\ln(q_T/Q)$.
- 🍎 All **equivalent** for *factorising* processes (such as inclusive Drell-Yan).

- 🍎 Dictionary:

$$\mathcal{H} = H C_1 C_2$$

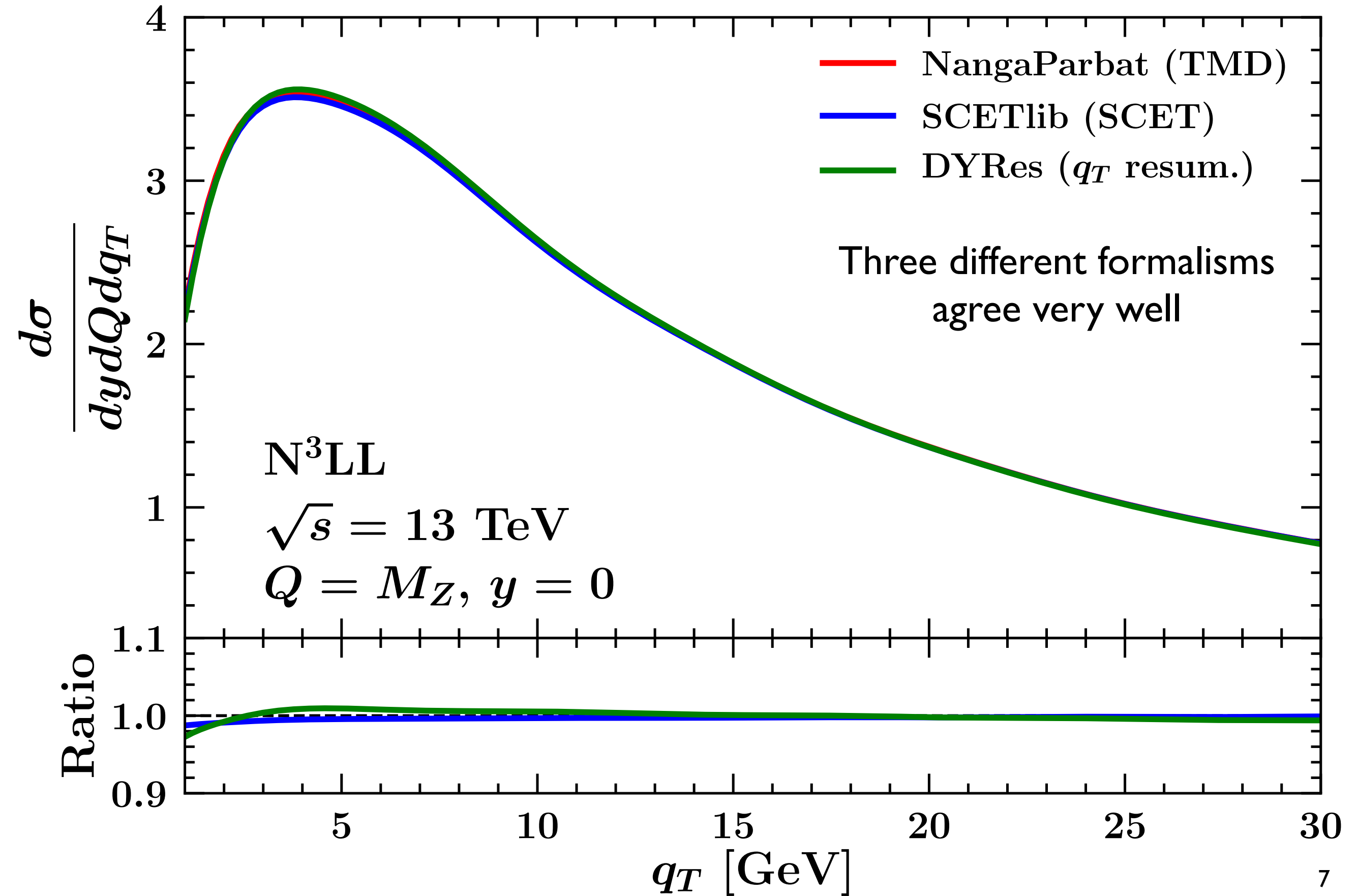
f_i : Collinear PDFs

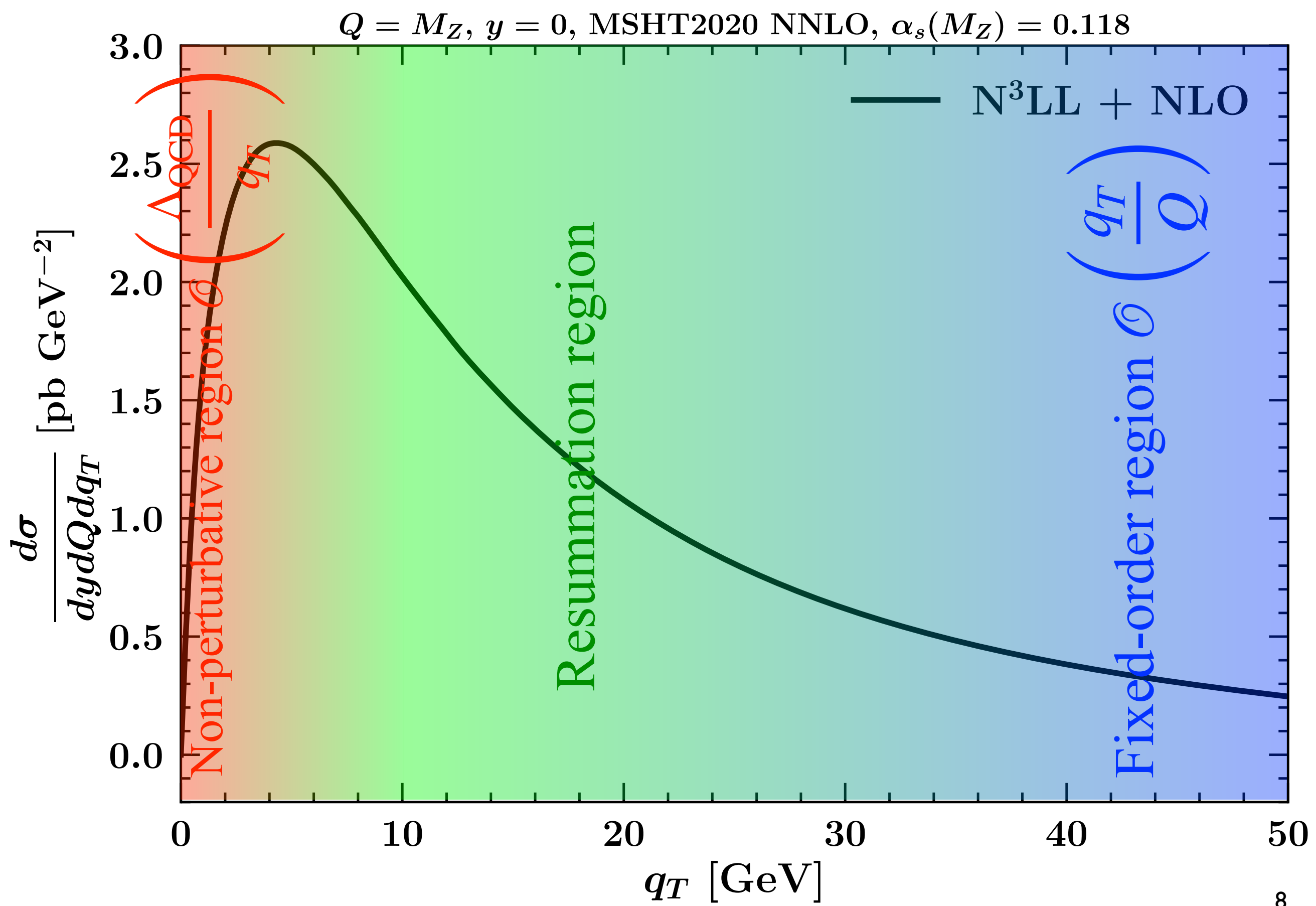
$$F_i = e^S C_i \otimes f_i$$

F_i : TMD PDFs

$$F_i = \sqrt{S} \times B_i$$

TMD, q_T resummation, SCET





Including $\mathcal{O}(q_T/Q)$ corrections

- 🍎 Accurate predictions for all $q_T \gg \Lambda_{\text{QCD}}$ can be obtained by **matching**:
 - 🍎 different **recipes** for the matching exist.

$$\left(\frac{d\sigma}{dq_T} \right)_{\text{match.}} = \left(\frac{d\sigma}{dq_T} \right)_{\text{res.}} + \left(\frac{d\sigma}{dq_T} \right)_{\text{f.o.}} - \left(\frac{d\sigma}{dq_T} \right)_{\text{d.c.}}$$

- 🍎 In order for the matching to actually take place one needs:

$$\left(\frac{d\sigma}{dq_T} \right)_{\text{res.}} \xrightarrow{\text{f.o.}} \left(\frac{d\sigma}{dq_T} \right)_{\text{d.c.}} \xleftarrow{q_T \ll Q} \left(\frac{d\sigma}{dq_T} \right)_{\text{f.o.}}$$

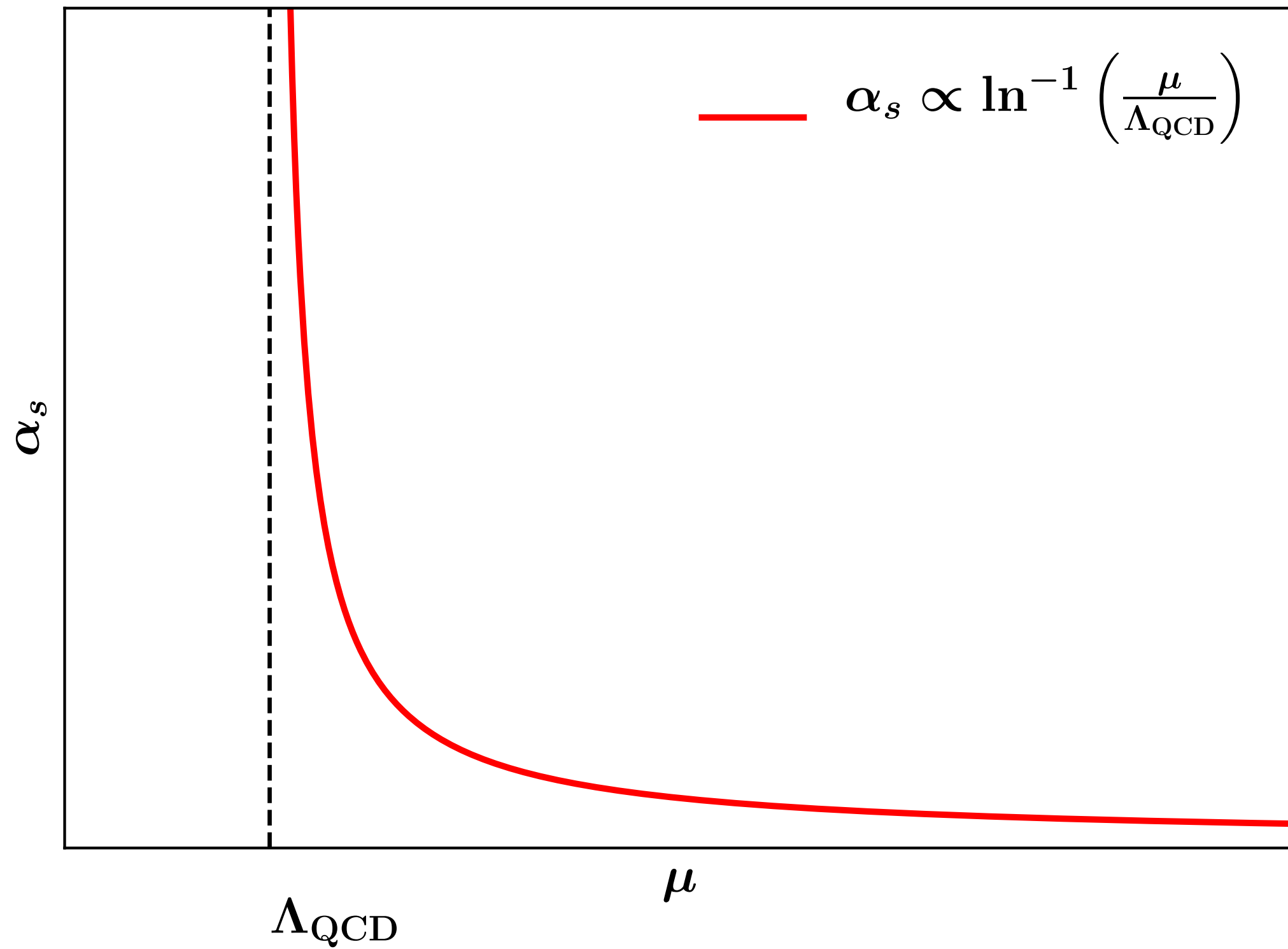
- 🍎 Fixed-order and double-counting terms obey **collinear factorisation**:

$$\left(\frac{d\sigma}{dq_T} \right)_{\text{f.o./d.c.}} = \int_0^1 dx_1 \int_0^1 dx_2 f_1(x_1, Q) f_2(x_2, Q) \left(\frac{d\hat{\sigma}}{dq_T} \right)_{\text{f.o./d.c.}}$$

Origin of $\mathcal{O}(\Lambda_{\text{QCD}}/q_T)$ corrections

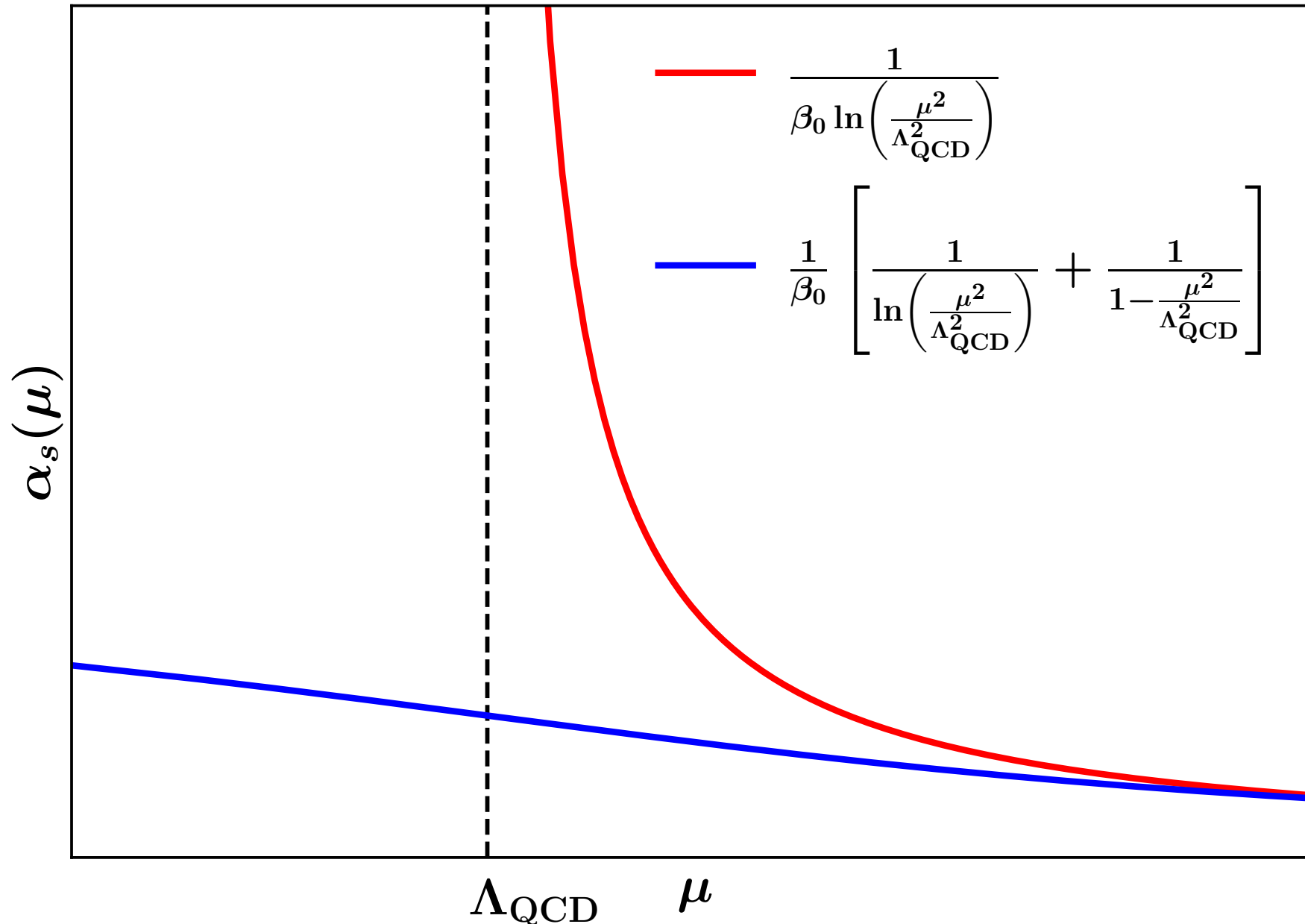
soft and/or collinear
radiation

$$\Rightarrow \sigma \propto \int_0^Q dk_T \alpha_s^p(k_T) \dots$$



Origin of $\mathcal{O}(\Lambda_{\text{QCD}}/q_T)$ corrections

- **Prescriptions** to avoid integrating over the **Landau pole** introduce power corrections $\mathcal{O}(\Lambda_{\text{QCD}}/q_T)$ of **non-perturbative origin**.
 - different prescriptions distribute these corrections differently.
- To see this, one can use a **dispersive** approach [Bogolyubov, Shirkov; Dokshitzer, Marchesini, Webber]:



Origin of $\mathcal{O}(\Lambda_{\text{QCD}}/q_T)$ corrections

- In the context of the resummation of logs of q_T , dispersive approaches have never been (seriously) considered.
- More popular approaches to the ***regularisation*** of the Landau pole are:
 - The **cutoff** method that leads to corrections that scale as $(\Lambda_{\text{QCD}}/q_T)^\alpha$.
In *direct space* (k_T) it amounts to:

$$\alpha_s(k_T) \rightarrow \alpha_s(\max[k_{T,\text{cutoff}}, k_T]) , \quad k_{T,\text{cutoff}} \gg \Lambda_{\text{QCD}}$$

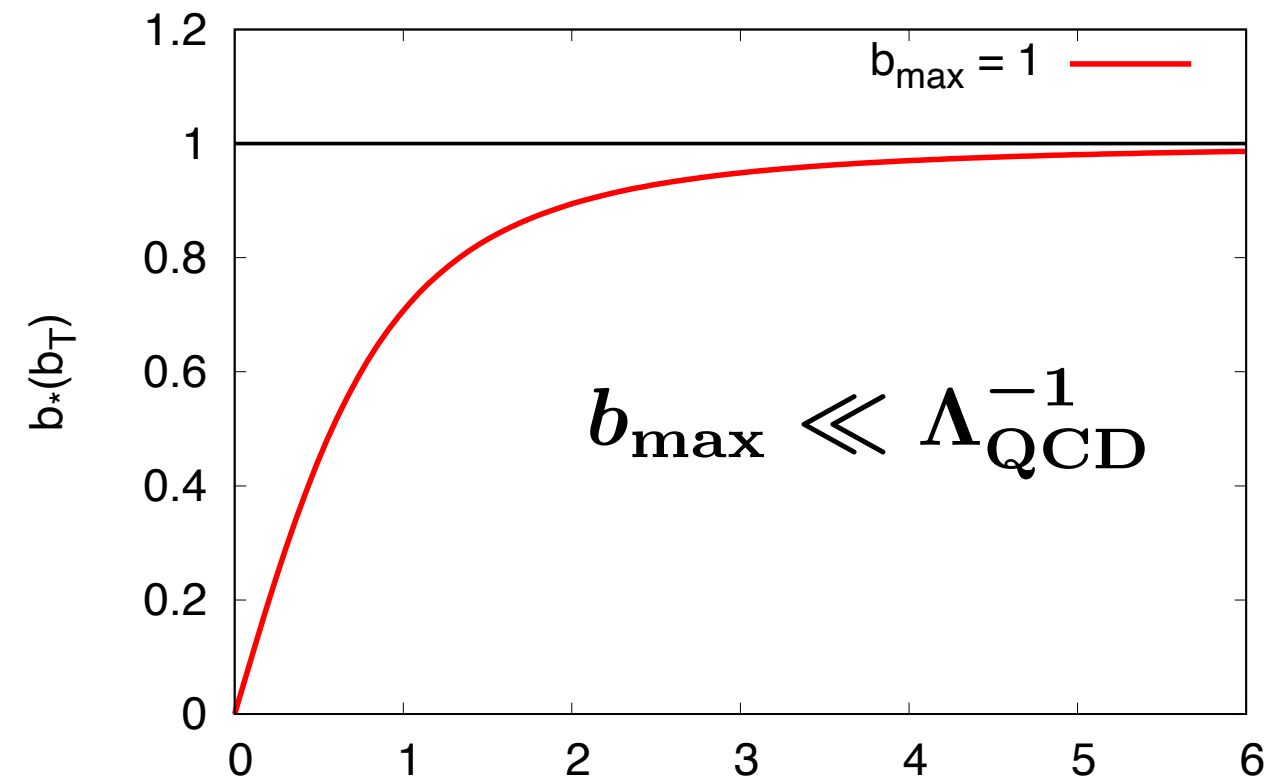
In *impact-parameter space* (b_T) it is typically implemented by means of the so-called ***b*-prescription***:

$$\alpha_s \left(\frac{2e^{-\gamma_E}}{b_T} \right) \rightarrow \alpha_s \left(\frac{2e^{-\gamma_E}}{b_*(b_T)} \right)$$

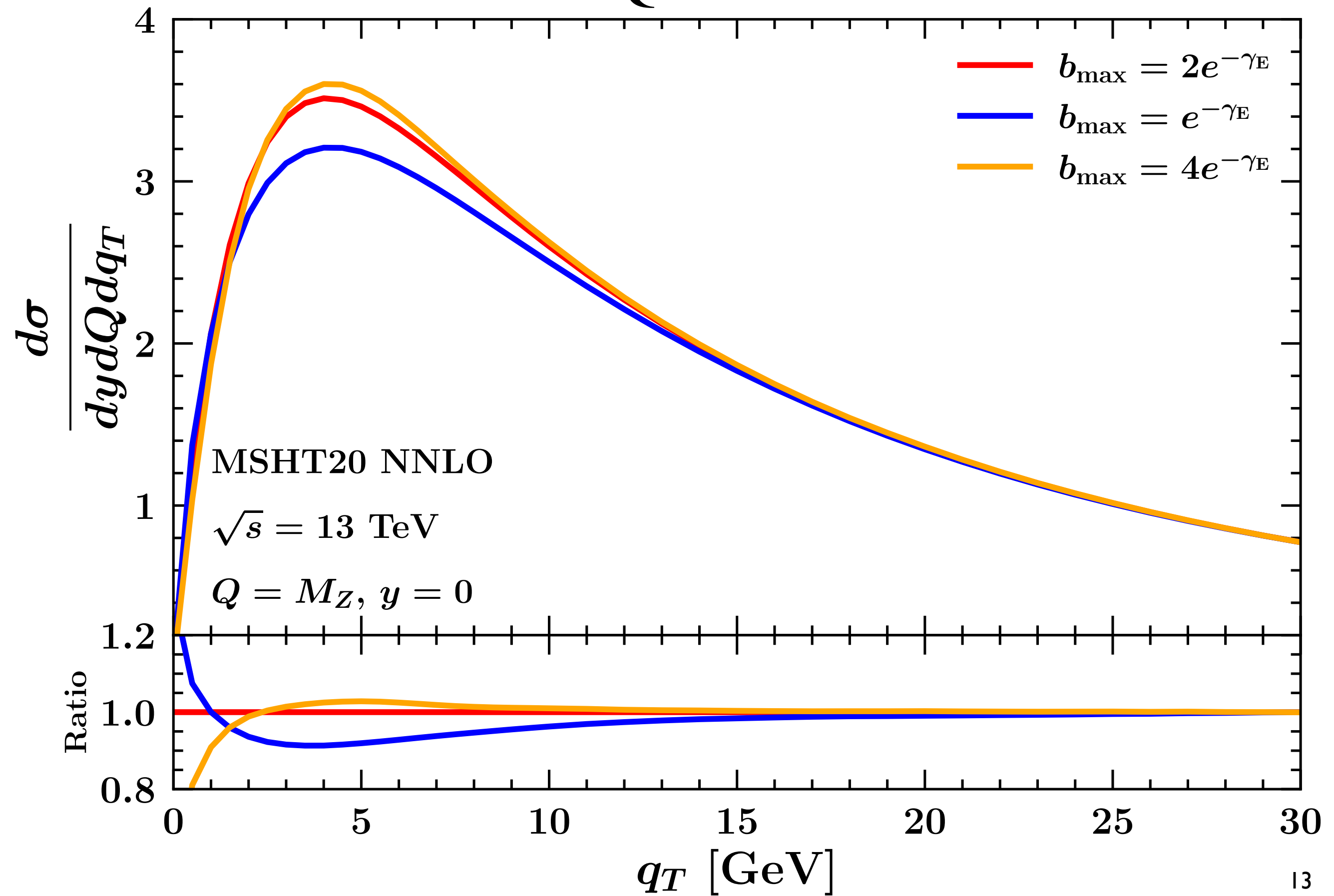
A classical choice is:

$$b_*(b_T) = \frac{b_T}{\sqrt{1 + b_T^2/b_{\max}^2}}$$

Scales below $b_{\max}^{-1} \sim k_{T,\text{cutoff}}$ are considered non-perturbative.



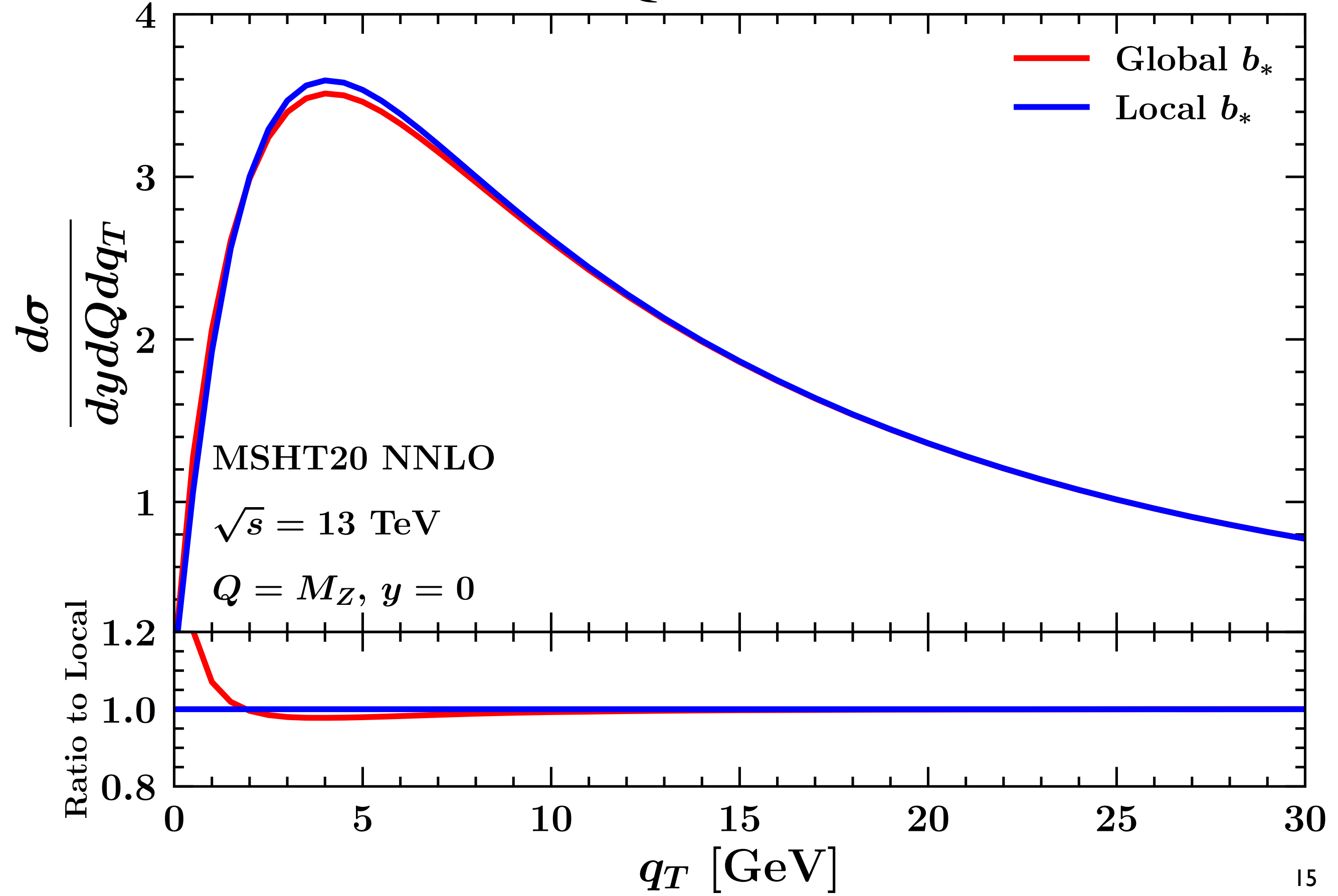
Origin of $\mathcal{O}(\Lambda_{\text{QCD}}/q_T)$ corrections



Origin of $\mathcal{O}(\Lambda_{\text{QCD}}/q_T)$ corrections

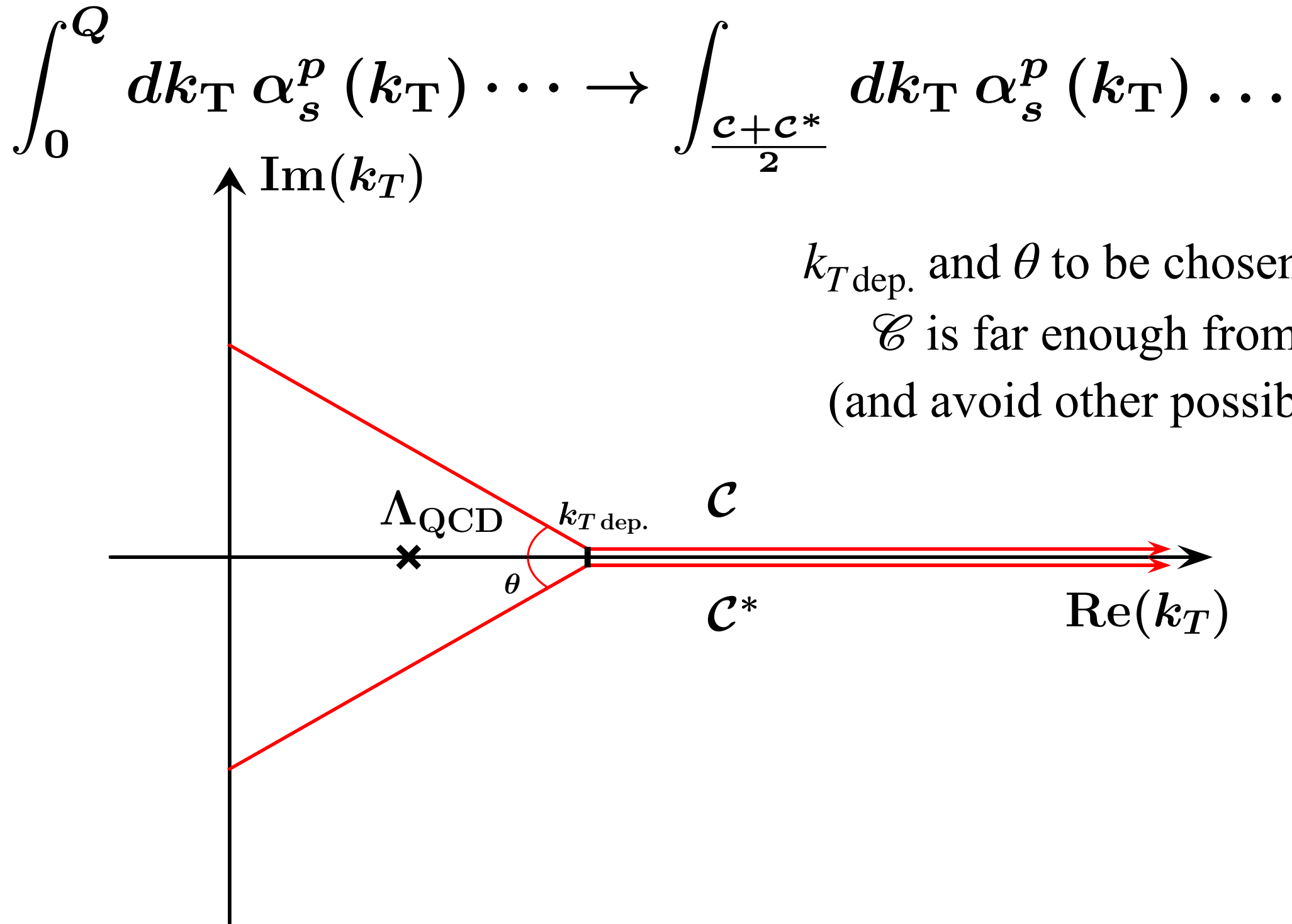
- 🍎 Within the context of the b_* prescription, **different recipes** exist:
 - 🍎 Replace $b_T \rightarrow b_*(b_T)$ everywhere in the calculation (including where it is not strictly needed to regulate the Landau pole) \Rightarrow **Global b_* prescription**
 - 🍎 Replace $b_T \rightarrow b_*(b_T)$ only where strictly need to regulate the Landau pole (*i.e.* in the running of α_s and PDFs) \Rightarrow **Local b_* prescription**

Origin of $\mathcal{O}(\Lambda_{\text{QCD}}/q_T)$ corrections



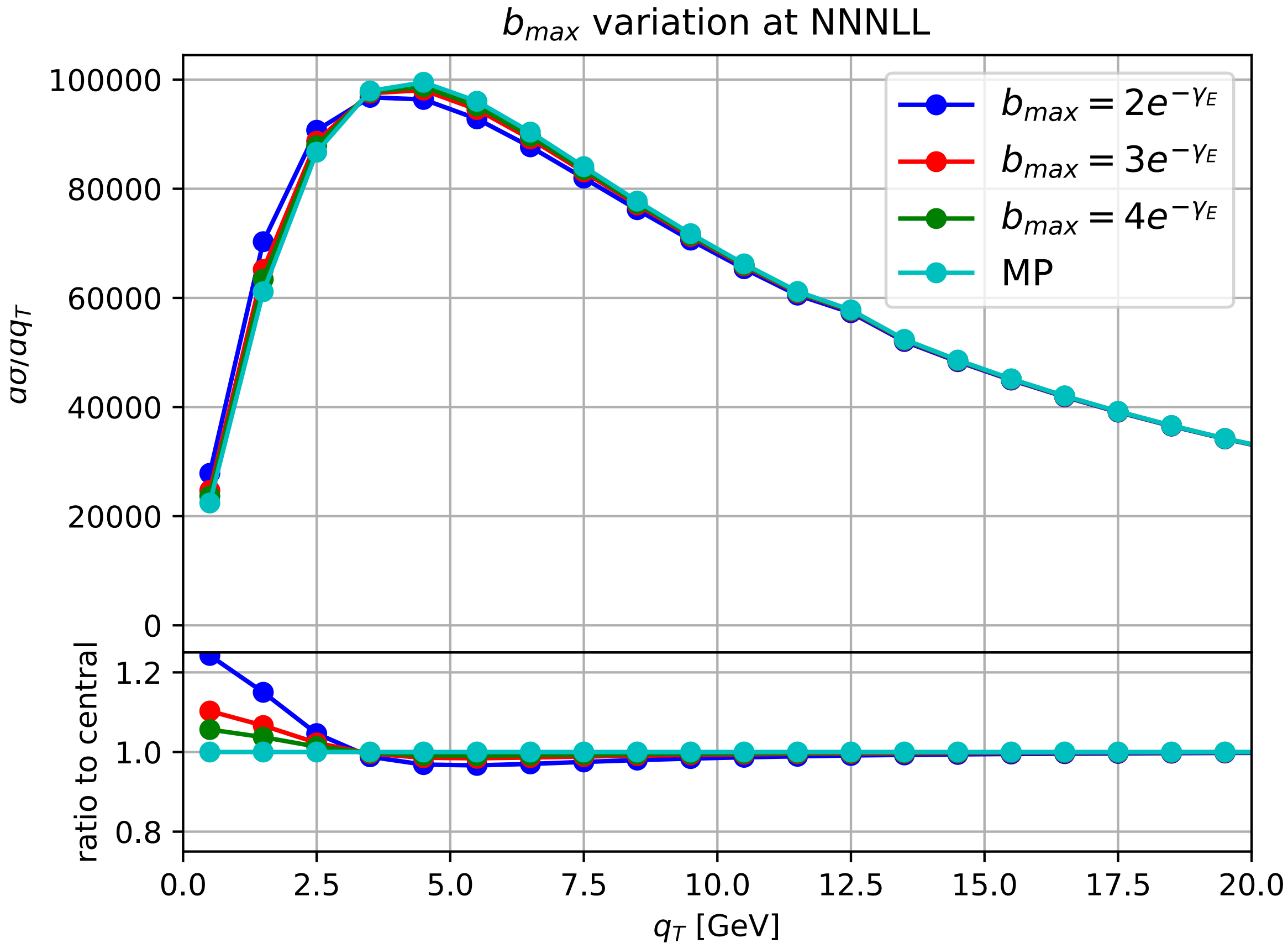
Origin of $\mathcal{O}(\Lambda_{\text{QCD}}/q_T)$ corrections

2) The **Minimal Prescription** [Catani, Mangano, Nason, Trentadue]:



The advantage of the MP is that non-perturbative corrections scale as $\exp[-\beta q_T/\Lambda_{\text{QCD}}]$, relegating them to smaller values of q_T .

Origin of $\mathcal{O}(\Lambda_{\text{QCD}}/q_T)$ corrections



Including $\mathcal{O}(\Lambda_{\text{QCD}}/q_T)$ corrections

- **TMD factorisation** is particularly suited to parametrise $\mathcal{O}(\Lambda_{\text{QCD}}/q_T)$ (non-perturbative) corrections:

Purely
Non-perturbative perturbative

$$F_i(x, b_T; \mu, \zeta) = \left[\frac{F_i(x, b_T; \mu, \zeta)}{F_i(x, \mathbf{b}_*(\mathbf{b}_T); \mu, \zeta)} \right] F_i(x, \mathbf{b}_*(\mathbf{b}_T); \mu, \zeta) \equiv f_{\text{NP}}^{(i)}(x, b_T; \zeta) F_i(x, \mathbf{b}_*(\mathbf{b}_T); \mu, \zeta)$$

- Properties of f_{NP} :

- it has to go to **one** as b_T goes to zero: reproduce the perturbative regime,
- it has to go to **zero** as b_T becomes large: mimic the Sudakov suppression,
- it does *not* depend on μ (ren. scale) but only on ζ (rapidity scale),
- it is generally **flavour dependent**,
- the ζ scaling is predictable, and flavour and x independent (Collins-Soper kernel).

- **Important:** f_{NP} is *not universal* as it depends on the specific \mathbf{b}_* or, more in general, on the strategy used to regularise the Landau pole.

Including $\mathcal{O}(\Lambda_{\text{QCD}}/q_T)$ corrections

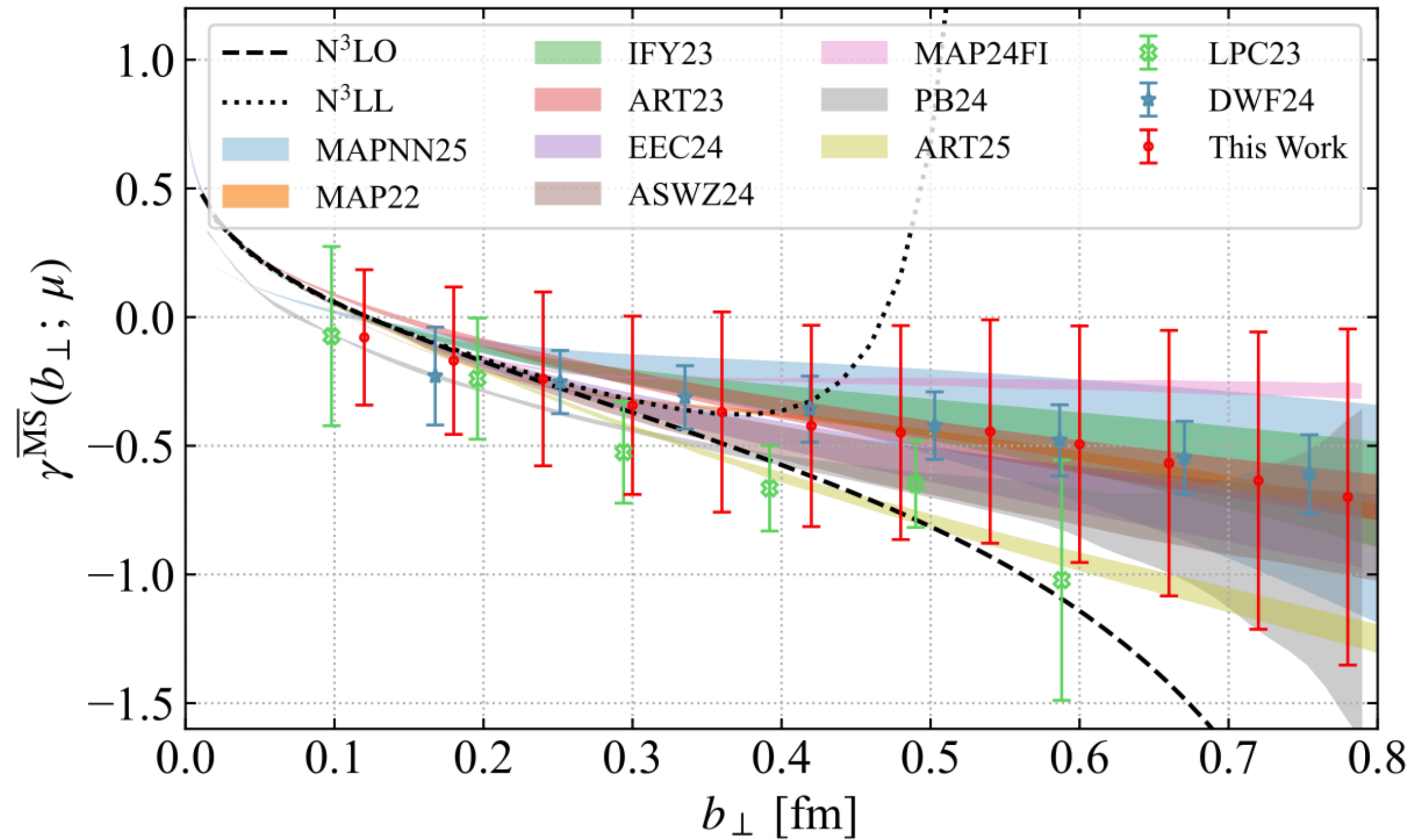
- Without loss of generality, f_{NP} can be parametrised as:

$$f_{\text{NP}}^{(i)}(x, b_T; \zeta) = \exp \left[-g_i(x, b_T) - g_K(b_T) \ln \left(\frac{\zeta}{Q_0^2} \right) \right]$$

- Given the properties above, there is not a huge latitude in defining f_{NP} :
 - both g_i and g_K have to go to zero as b_T tends to zero, and become large as b_T becomes large:
 - f_{NP} can be sensibly different from one only for $b_T^{-1} \lesssim \Lambda_{\text{QCD}}^{-1}$ ($k_T \lesssim \Lambda_{\text{QCD}}$).
 - g_K (non-perturbative contribution to the Collins-Soper kernel) can be determined faithfully having a **large lever arm** in $\zeta \propto Q$:
 - both **low and high invariant-mass data** necessary.
 - Lattice** simulations available.

Collis-Soper kernel

[2504.04625]



Importance of the x -dependence

- However f_{NP} cannot be too simple either!
- In [JHEP 07 (2020) 117] a fit of an **x -dependent** f_{NP} to a set 353 DY data points was done, obtaining a χ^2 per data point (χ^2/N_{dat}) equal to **1.02**:
- A **gaussian, x -independent** f_{NP} was also tested:

$$f_{\text{NP}}^{\text{DWS}}(b_T, \zeta) = \exp \left[-\frac{1}{2} \left(g_1 + g_2 \ln \left(\frac{\zeta}{2Q_0^2} \right) \right) b_T^2 \right]$$

- This f_{NP} was used to fit the full data set as well as a subset in which rapidity-dependent data (from ATLAS) was excluded:

	Full dataset	No y -differential data
Global χ^2/N_{dat}	1.339	0.895

- Gaussian ansatz is insufficient** to describe data accurately.
Deterioration largely due to the rapidity-dependent data.

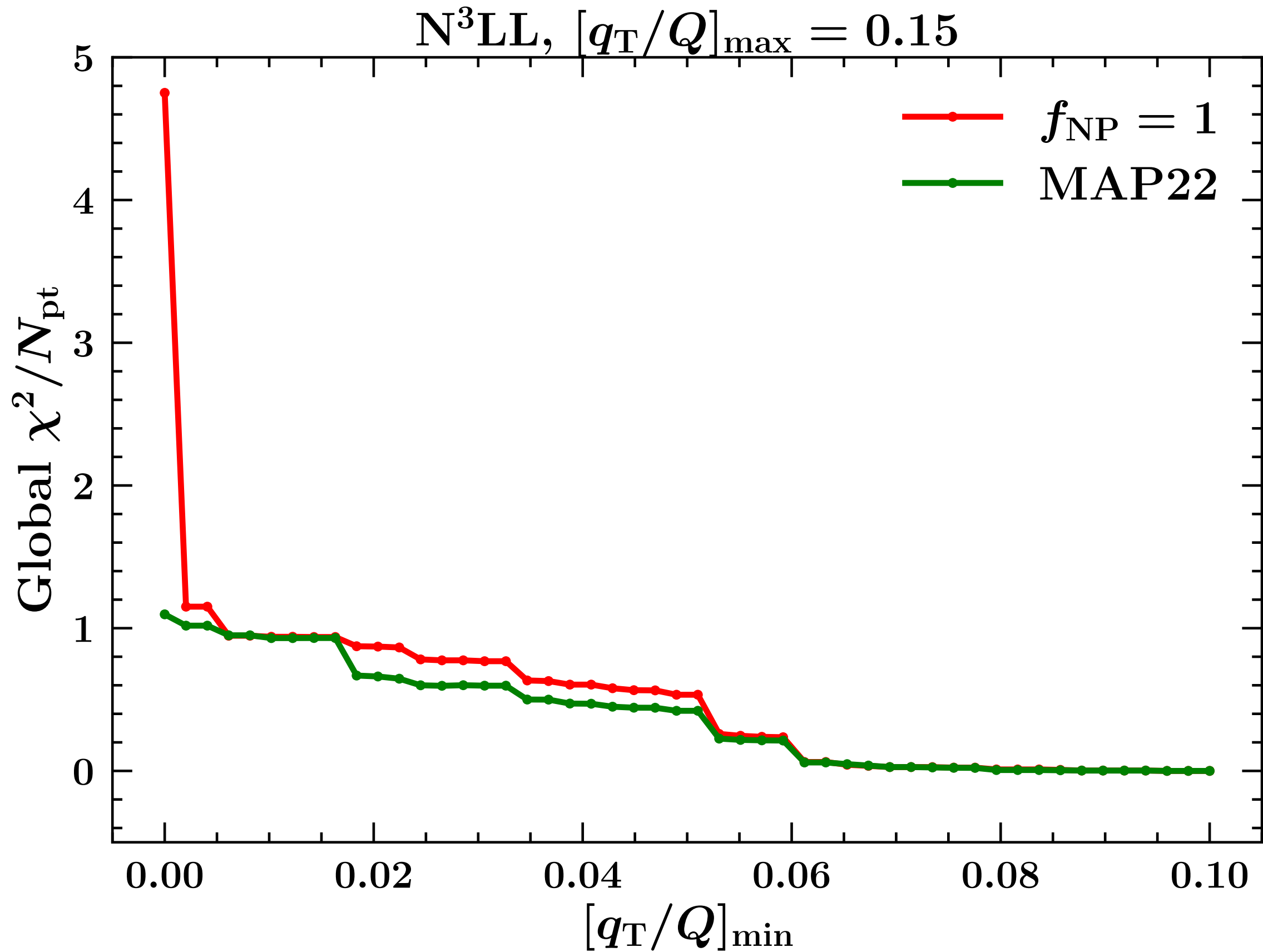
Relevance of f_{NP} at high-energies

- 🍎 In order to assess the relevance of f_{NP} for the description of data at high-energy colliders (Tevatron and LHC), compute the χ^2 of predictions:
 - 1) setting $f_{\text{NP}} = 1$,
 - 2) using a fit for f_{NP} (e.g. MAP22 [*JHEP 10 (2022) 127*]).
- 🍎 The theoretical accuracy is $N^3 LL$.
- 🍎 The χ^2 accounts for all systematic uncertainties (correlated and uncorrelated) and for collinear PDF uncertainties (MSHT2020).
- 🍎 A cut $q_T/Q < [q_T/Q]_{\text{max}} = 0.15$ is enforced to ensure to be in the resummation region,
- 🍎 A cut $q_T/Q > [q_T/Q]_{\text{min}} \in [0, 0.1]$ is also enforced to verify that f_{NP} plays a more prominent role for $q_T \lesssim \Lambda_{QCD} \sim 1 - 2 \text{ GeV}$.

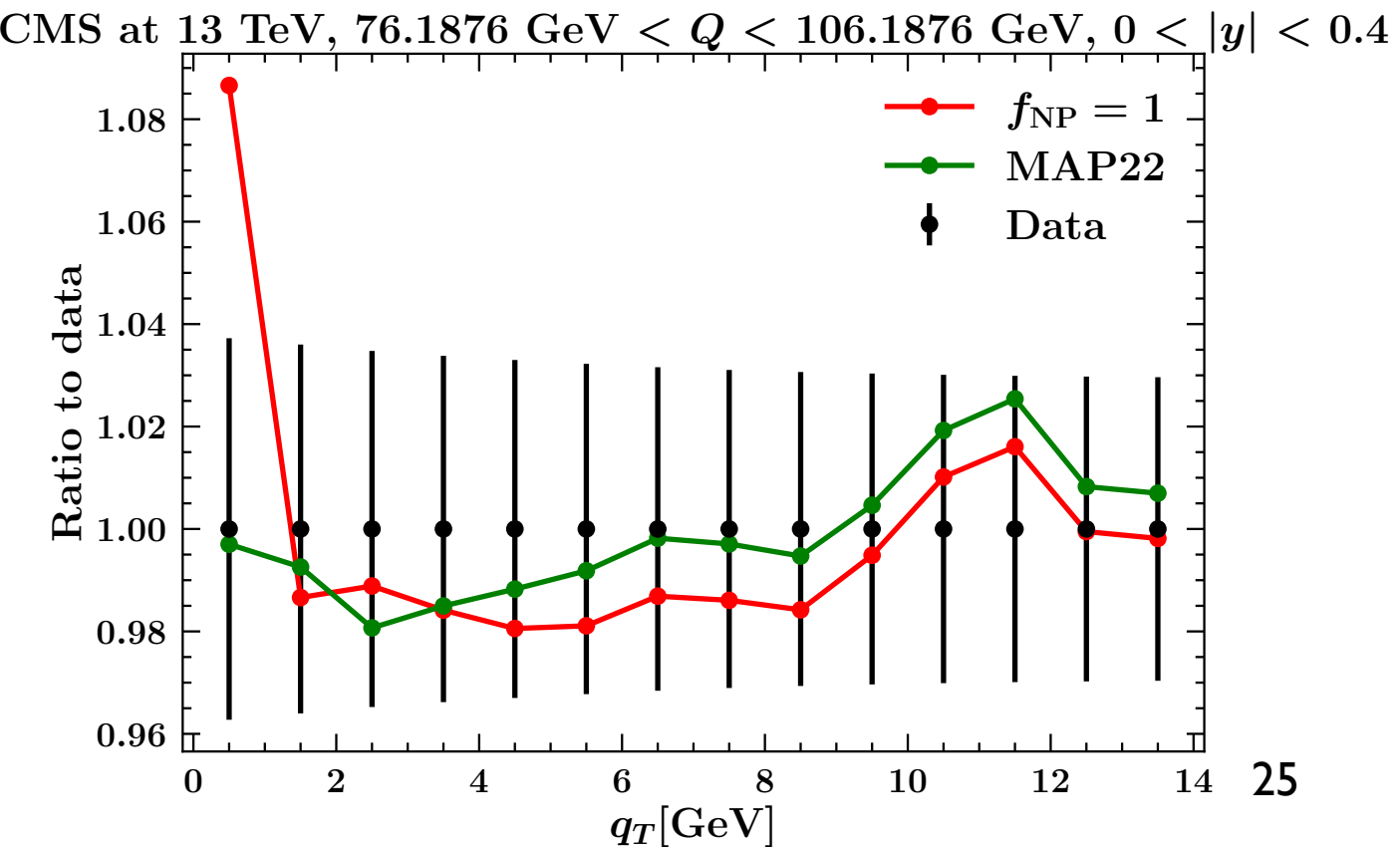
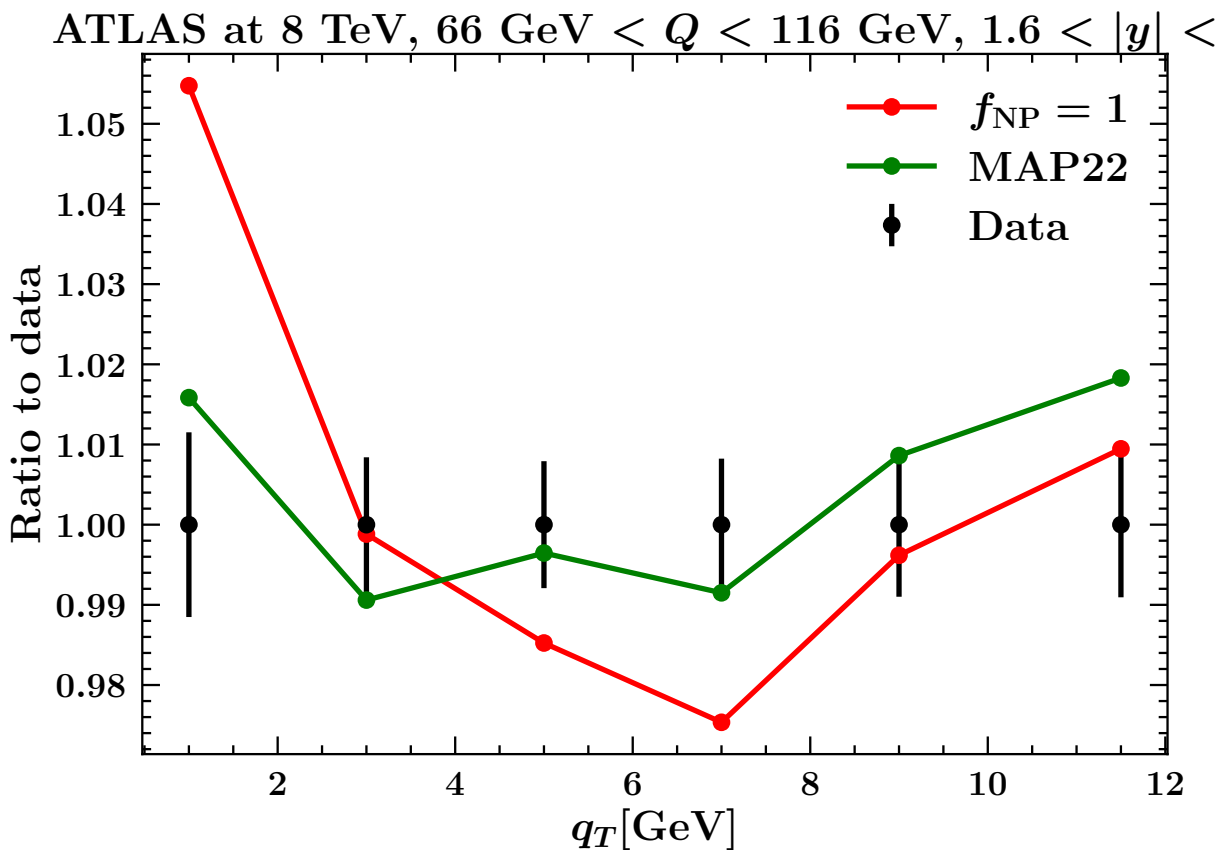
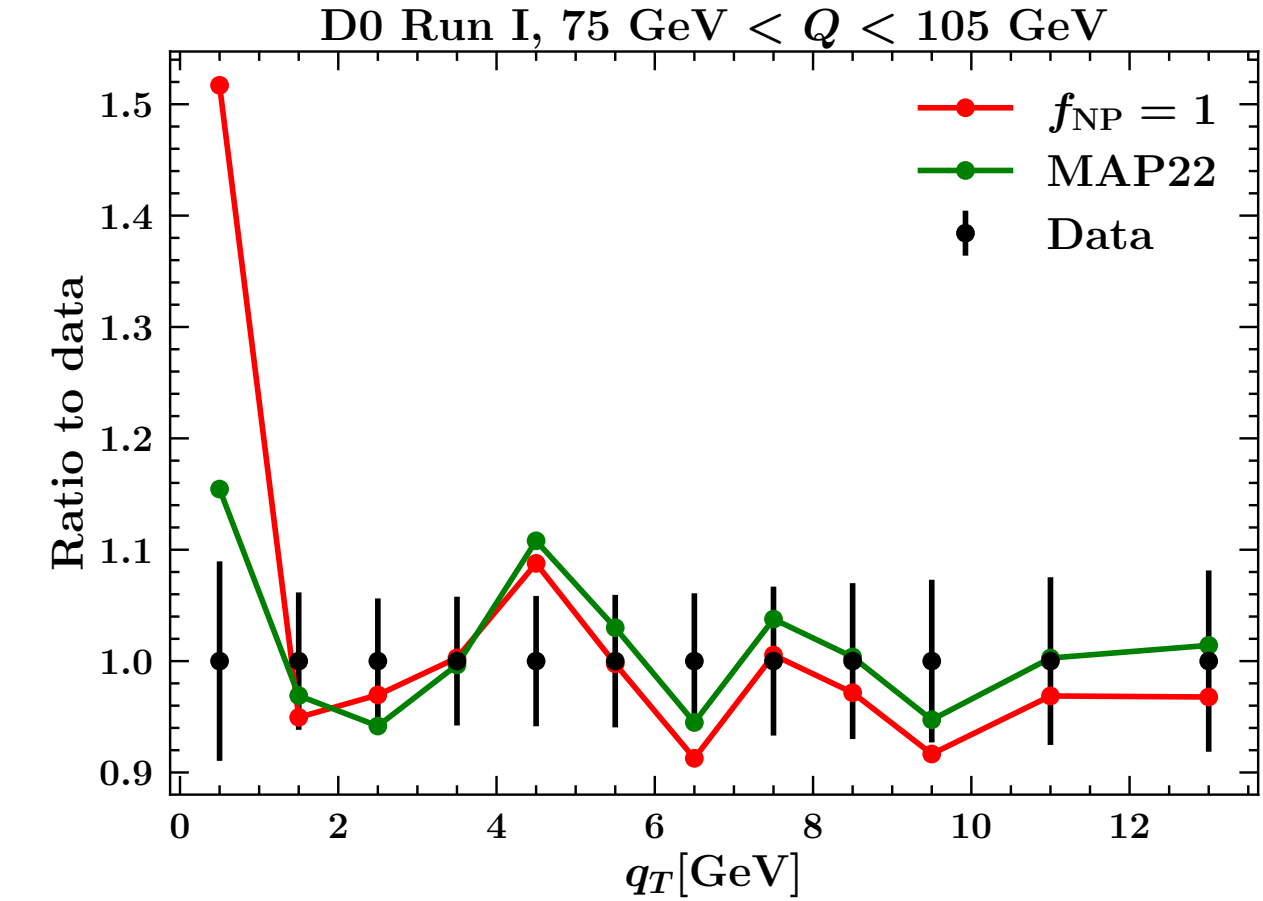
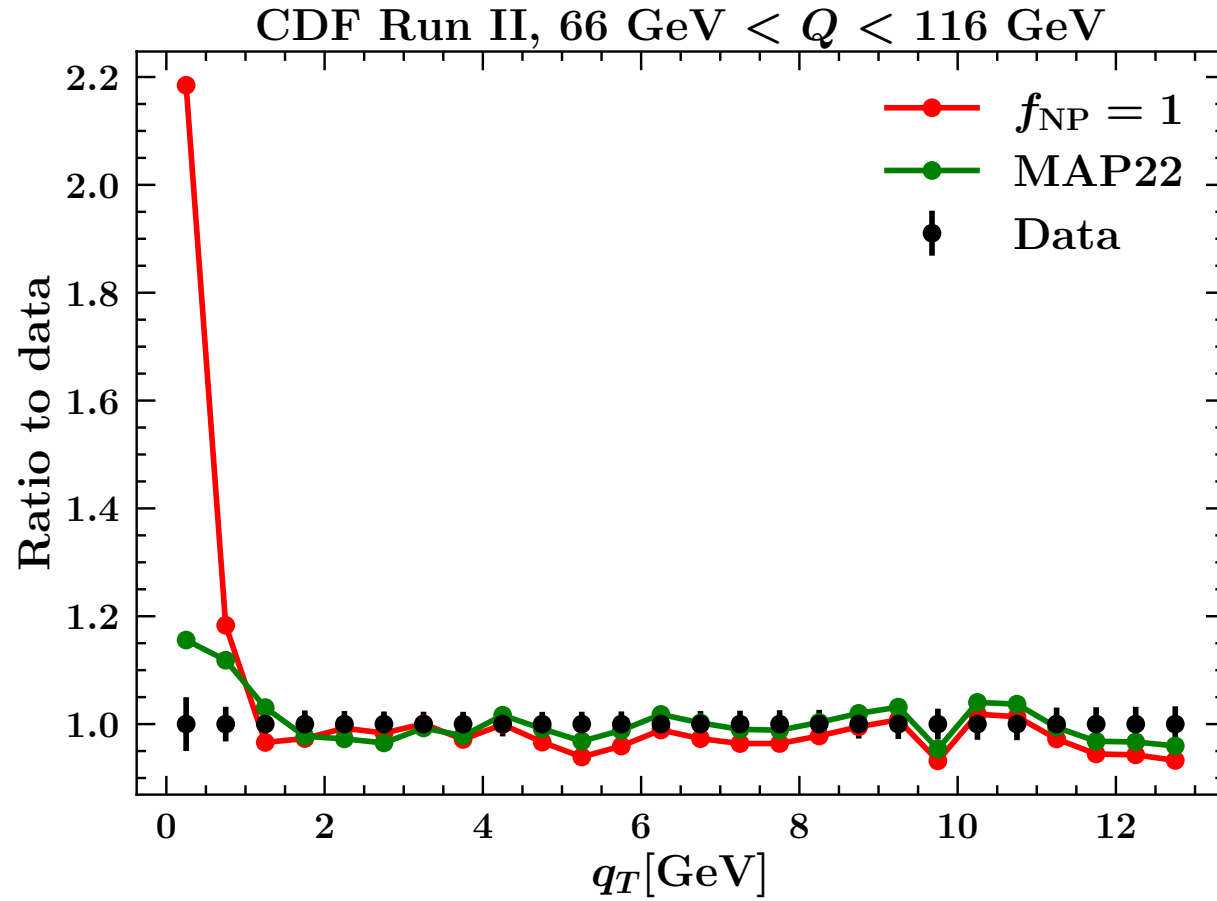
Relevance of f_{NP} at high-energies

Experiment	Observable	\sqrt{s} [GeV]	Q [GeV]	y	Lepton cuts
CDF Run I	$d\sigma/d \mathbf{q}_T $	1800	66 - 116	Inclusive	-
CDF Run II	$d\sigma/d \mathbf{q}_T $	1960	66 - 116	Inclusive	-
D0 Run I	$d\sigma/d \mathbf{q}_T $	1800	75 - 105	Inclusive	-
D0 Run II	$(1/\sigma)d\sigma/d \mathbf{q}_T $	1960	70 - 110	Inclusive	-
D0 Run II (μ)	$(1/\sigma)d\sigma/d \mathbf{q}_T $	1960	65 - 115	$ y < 1.7$	$p_{T\ell} > 15 \text{ GeV}$ $ \eta_\ell < 1.7$
LHCb 7 TeV	$d\sigma/d \mathbf{q}_T $	7000	60 - 120	$2 < y < 4.5$	$p_{T\ell} > 20 \text{ GeV}$ $2 < \eta_\ell < 4.5$
LHCb 8 TeV	$d\sigma/d \mathbf{q}_T $	8000	60 - 120	$2 < y < 4.5$	$p_{T\ell} > 20 \text{ GeV}$ $2 < \eta_\ell < 4.5$
LHCb 13 TeV	$d\sigma/d \mathbf{q}_T $	13000	60 - 120	$2 < y < 4.5$	$p_{T\ell} > 20 \text{ GeV}$ $2 < \eta_\ell < 4.5$
CMS 7 TeV	$(1/\sigma)d\sigma/d \mathbf{q}_T $	7000	60 - 120	$ y < 2.1$	$p_{T\ell} > 20 \text{ GeV}$ $ \eta_\ell < 2.1$
CMS 8 TeV	$(1/\sigma)d\sigma/d \mathbf{q}_T $	8000	60 - 120	$ y < 2.1$	$p_{T\ell} > 15 \text{ GeV}$ $ \eta_\ell < 2.1$
CMS 13 TeV	$d\sigma/d \mathbf{q}_T $	13000	76 - 106	$ y < 0.4$ $0.4 < y < 0.8$ $0.8 < y < 1.2$ $1.2 < y < 1.6$ $1.6 < y < 2.4$	$p_{T\ell} > 25 \text{ GeV}$ $ \eta_\ell < 2.4$
ATLAS 7 TeV	$(1/\sigma)d\sigma/d \mathbf{q}_T $	7000	66 - 116	$ y < 1$ $1 < y < 2$ $2 < y < 2.4$	$p_{T\ell} > 20 \text{ GeV}$ $ \eta_\ell < 2.4$
ATLAS 8 TeV on-peak	$(1/\sigma)d\sigma/d \mathbf{q}_T $	8000	66 - 116	$ y < 0.4$ $0.4 < y < 0.8$ $0.8 < y < 1.2$ $1.2 < y < 1.6$ $1.6 < y < 2$ $2 < y < 2.4$	$p_{T\ell} > 20 \text{ GeV}$ $ \eta_\ell < 2.4$
ATLAS 8 TeV off-peak	$(1/\sigma)d\sigma/d \mathbf{q}_T $	8000	46 - 66 116 - 150	$ y < 2.4$	$p_{T\ell} > 20 \text{ GeV}$ $ \eta_\ell < 2.4$
ATLAS 13 TeV	$(1/\sigma)d\sigma/d \mathbf{q}_T $	13000	66 - 113	$ y < 2.5$	$p_{T\ell} > 27 \text{ GeV}$ $ \eta_\ell < 2.5$

Relevance of f_{NP} at high-energies



Relevance of f_{NP} at high-energies



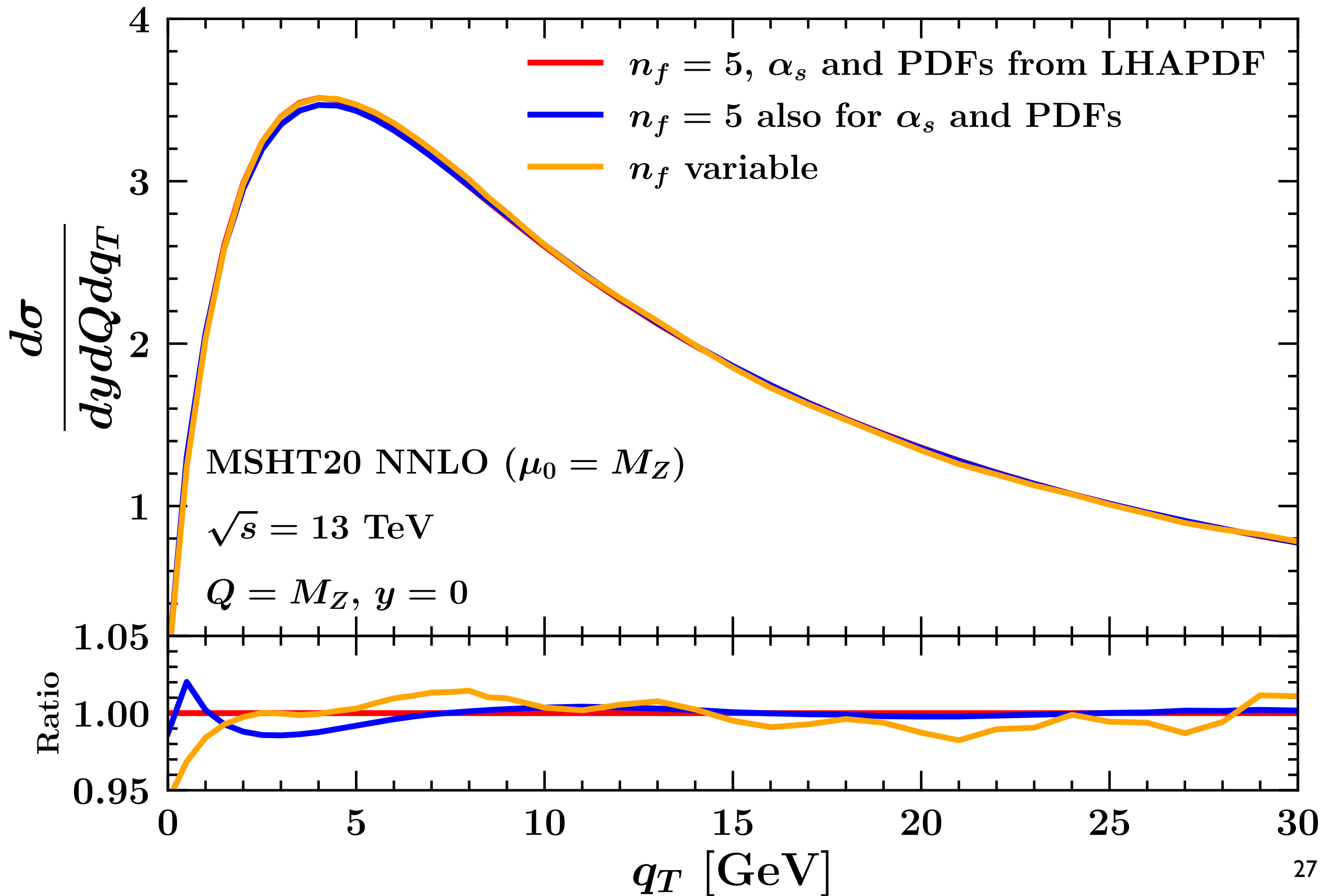
Heavy-quark masses/thresholds

- 🍎 Usually, the resummation of logs of q_T does not account for the finiteness of **heavy-quark (charm and bottom) masses** m_h :
 - 🍎 a fully consistent calculation accounting for heavy-quark masses is hard to achieve,
 - 🍎 however these affects are expected to be relevant when $q_T \lesssim m_h$.
- 🍎 Indeed, most of the calculations are performed in the **massless** scheme.
- 🍎 The massless scheme introduces an explicit dependence of the relevant quantities on the number of active flavours n_f :
 - 🍎 a partial account of heavy-quark mass effects can be achieved by **varying** n_f at the heavy-quark thresholds depending on the scale at which each quantity is computed.
- 🍎 For example:

$$F^{(4)}(\mu) = e^{S^{(4)}(\mu, m_h)} e^{S^{(3)}(m_h, \mu_b)} [C^{(3)} \otimes f^{(3)}](\mu_b), \quad \mu_b < m_h < \mu$$

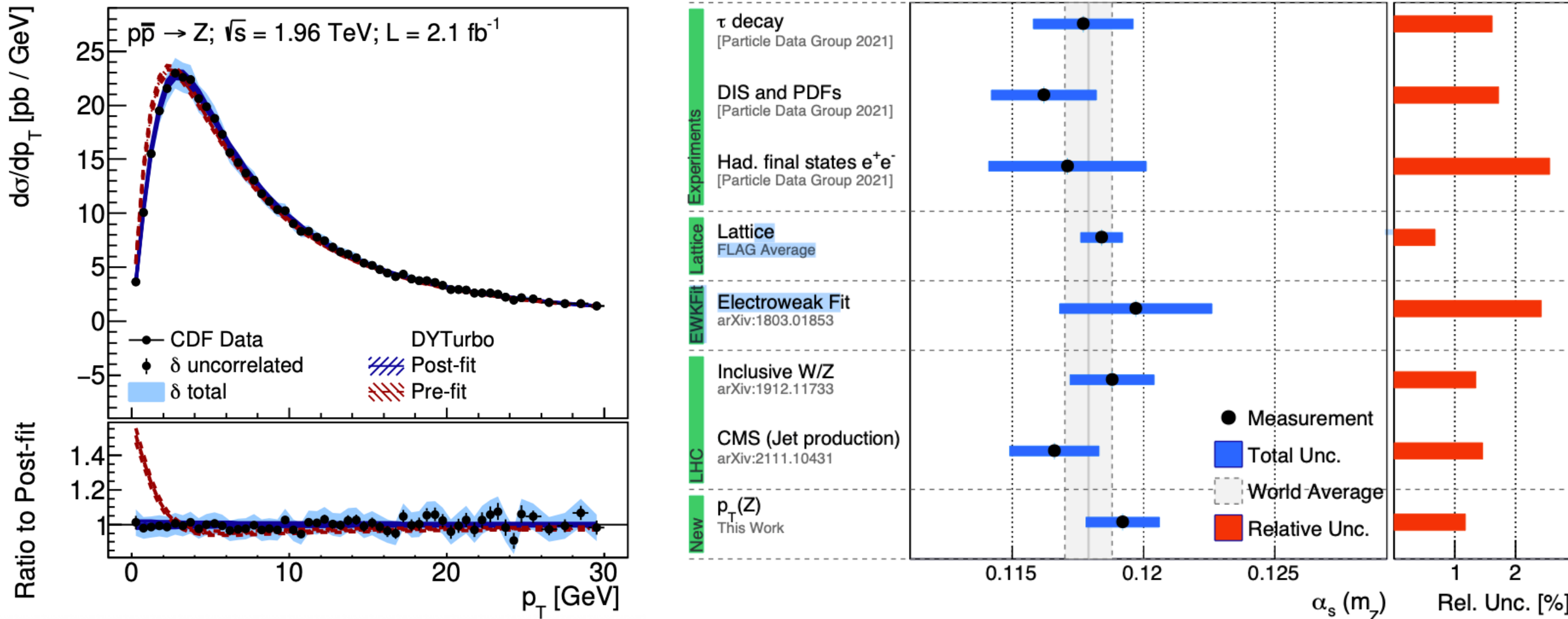
- 🍎 where $\mu_b = b_0/b_T$ with b_T to be integrated over.

Heavy-quark masses/thresholds



TMDs and the strong coupling

- 🍎 A recent paper [[2203.05394](#)], has demonstrated a *strong* sensitivity of the low- q_T Drell-Yan spectrum to α_s ($\alpha_s(M_Z) = 0.1191^{+0.0013}_{-0.0016}$).



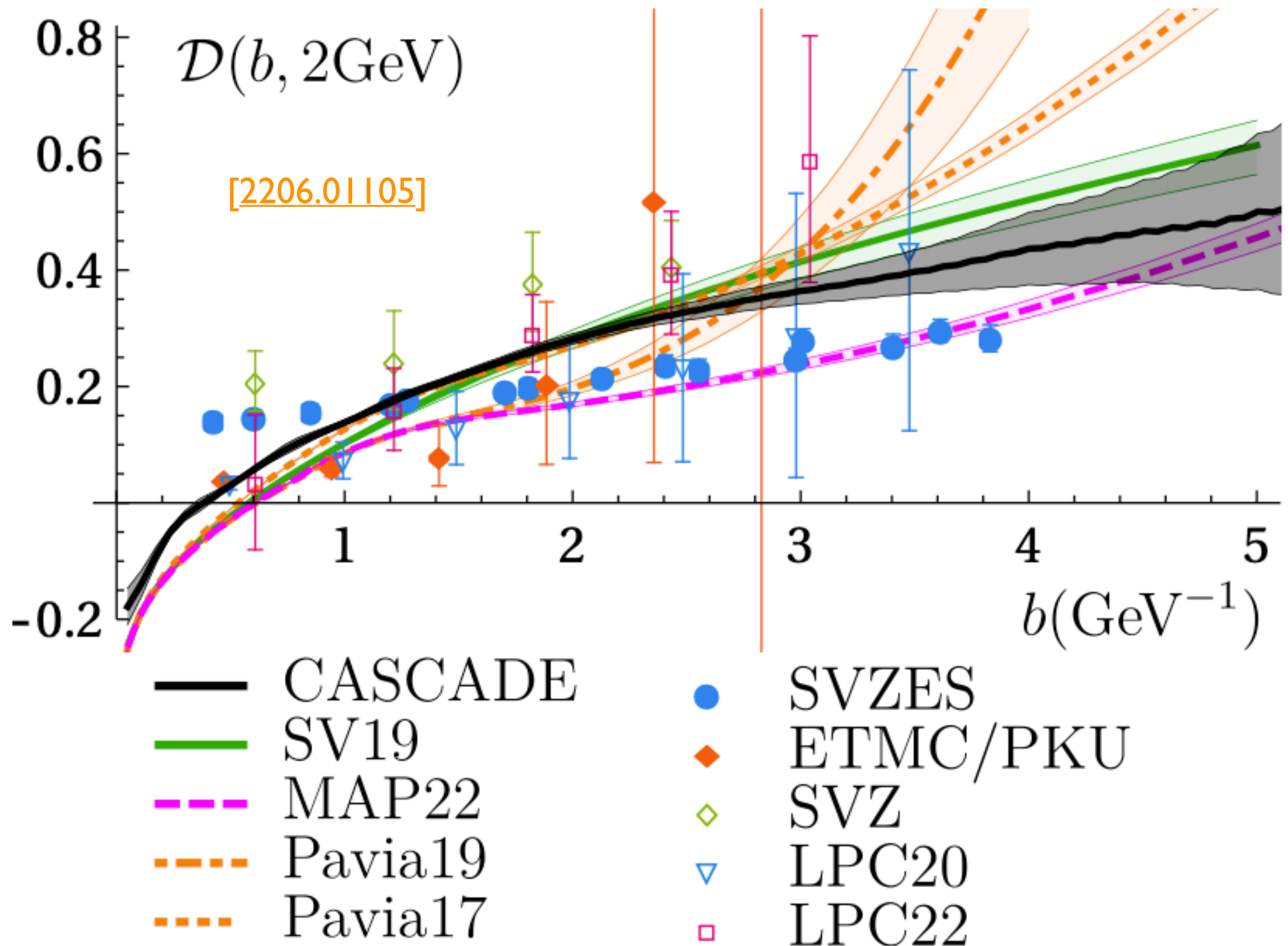
- 🍎 Importantly, this work has required a determination of the non-perturbative component of TMDs.
- 🍎 Work based of Tevatron (CDF) data \Rightarrow huge **potential of the LHC** (see [[ATLAS CONF Note](#)]).

Conclusions

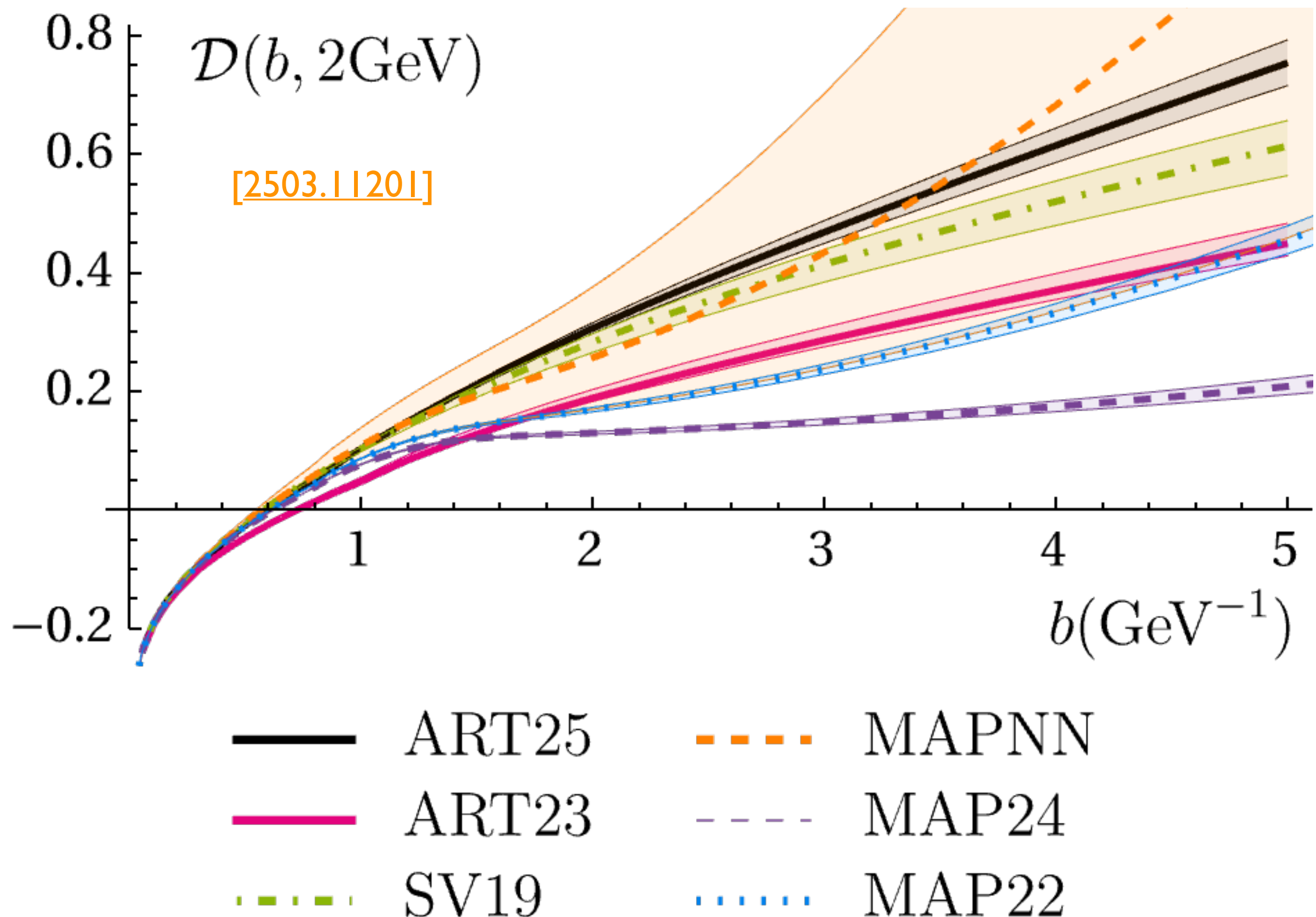
- 🍎 **Non perturbative effects** that scale like a power of Λ_{QCD}/q_T are sizeable at small q_T , which is the domain of resummation,
- 🍎 necessary to describe the first bins in q_T of high-energy data,
- 🍎 **TMD factorisation** is just one of the possible ways to resum large logs of q_T , but it is particularly suited to study non-perturbative effects.
- 🍎 Within TMD factorisation, different **extractions from data** of these effects as encoded in f_{NP} exist (not discussed in detail here).
- 🍎 In doing so, several aspects have to be considered:
 - 🍎 regularisation, parameterisation of f_{NP} , flavour dependence, (heavy quarks), etc.
 - 🍎 All of them have to be accounted for to achieve reliable predictions for the $Z q_T$, which affects the precision of the **W mass** determination.

Backup

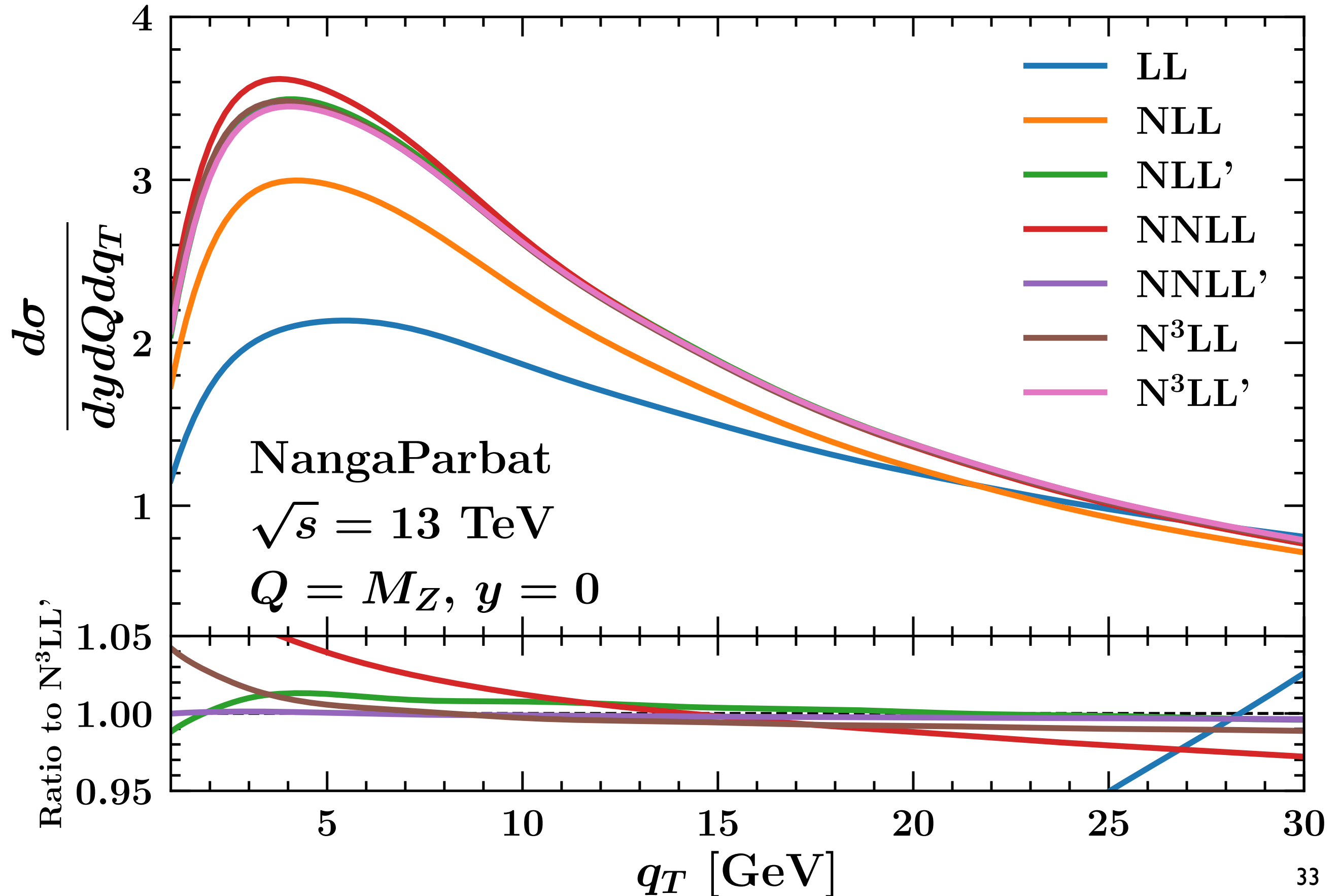
Collis-Soper kernel



Collis-Soper kernel



Perturbative convergence



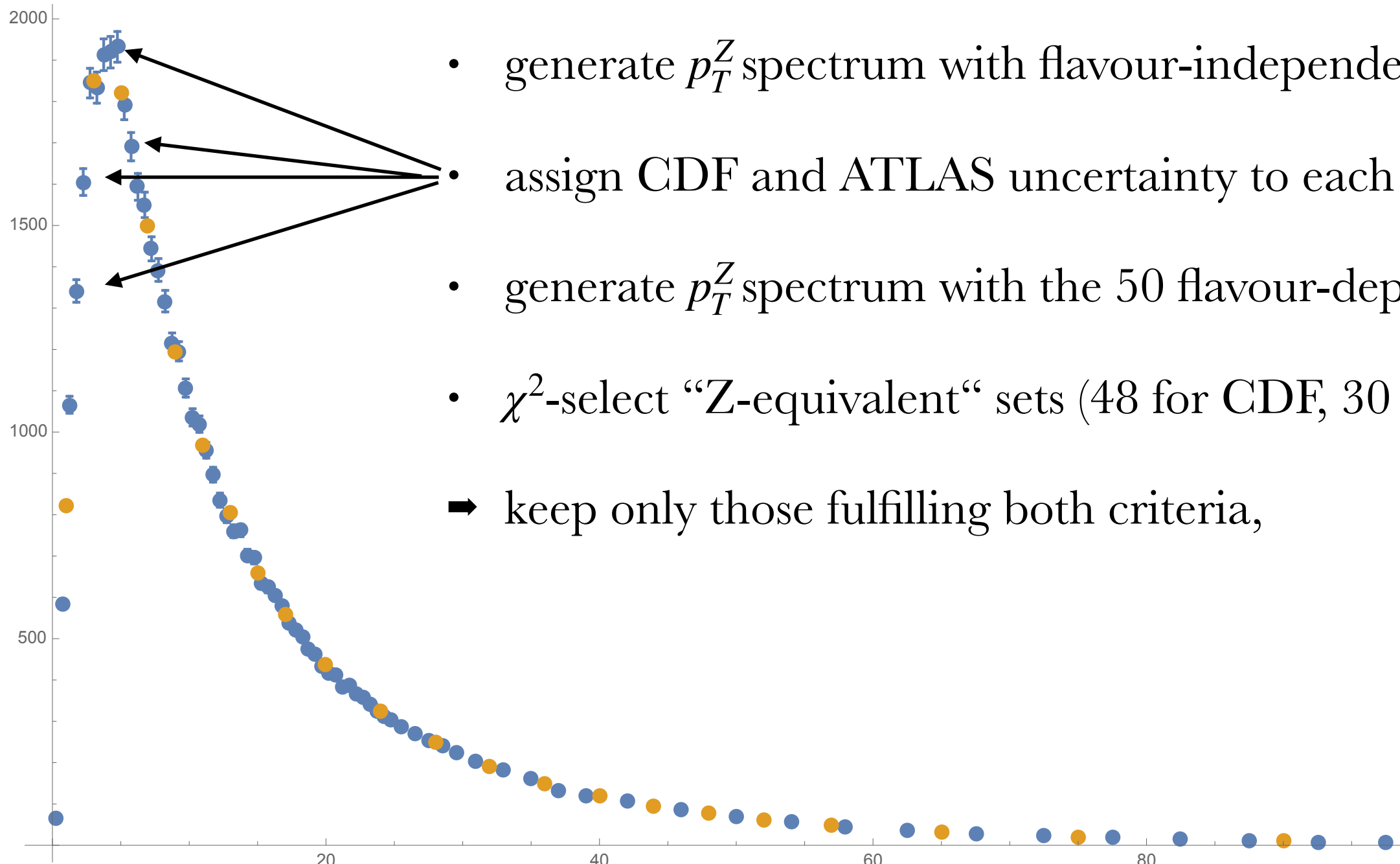
Flavour dependence of f_{NP}

- 🍎 For each TMD use a **Gaussian ansatz**:

$$f_{\text{NP}}(b_T, \zeta) = \exp \left[-g_a b_T^2 - g_K b_T^2 \ln \left(\frac{\zeta}{Q_0^2} \right) \right]$$

- 🍎 **1 flavour-independent set** with $g_a = 0.4 \text{ GeV}^2$, [Guzzi, Nadolsky, Wang (2014)]
- 🍎 **50 flavour-dependent sets** with $\{g_{u_\nu}, g_{d_\nu}, g_{u_s}, g_{d_s}, g_s\}$, $g_a \in [0.2, 0.6] \text{ GeV}^2$,
- 🍎 keep g_K fixed. [Bacchetta, Delcarro, Pisano, Radici, Signori (2017)]

“Z-equivalent” sets



Impact on m_W

- Take the “Z-equivalent” *flavour-dependent* parameter sets and compute *low-statistics* (135M) m_T, p_T^l, p_T^ν distributions

→ **pseudodata**

- Take the *flavour-independent* parameter set and compute *high-statistics* (750M) m_T, p_T^l, p_T^ν distributions for 30 different values of M_W

→ **templates**

- perform the template fit procedure and compute the shifts induced by flavour effects**

- transverse mass: zero or few MeV shifts, generally favouring lower values for W^- (**preferred by EW fit**)

- lepton pt: quite important shifts (envelope **up to 15 MeV**)

- neutrino pt: same order of magnitude (or bigger) as lepton pt

Set	ΔM_{W+}			ΔM_{W-}		
	m_T	$p_{T\ell}$	$p_{T\nu}$	m_T	$p_{T\ell}$	$p_{T\nu}$
1	0	-1	-2	-2	3	-3
2	0	-6	0	-2	0	-5
3	-1	9	0	-2	4	-10
4	0	0	-2	-2	-4	-10
5	0	4	1	-1	-3	-6
6	1	0	2	-1	4	-4
7	2	-1	2	-1	0	-8
8	0	2	8	1	7	8
9	0	4	-3	-1	0	7

TABLE I: ATLAS 7 TeV

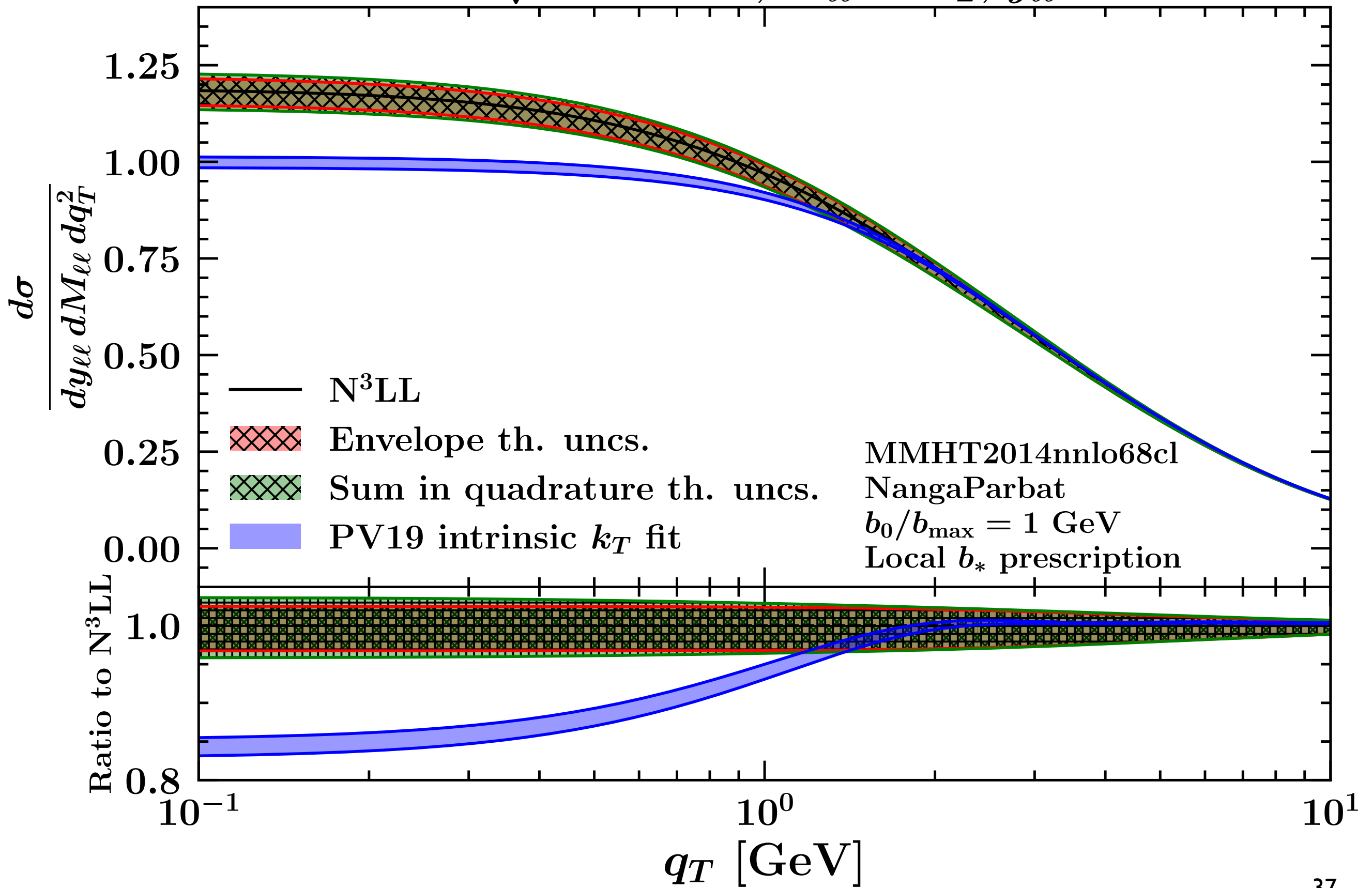
Set	ΔM_{W+}			ΔM_{W-}		
	m_T	$p_{T\ell}$	$p_{T\nu}$	m_T	$p_{T\ell}$	$p_{T\nu}$
1	-1	-5	7	-1	-3	8
2	-1	-15	6	0	5	10
3	-1	1	8	-1	-7	5
4	-1	-15	6	0	-4	5
5	-1	-4	6	-1	-7	5
6	-1	-5	7	0	2	9
7	-1	-15	6	-1	-6	5
8	-1	0	8	0	3	10
9	-1	-7	7	0	4	10

TABLE II: LHCb 13 TeV

Set	u_v	d_v	u_s	d_s	s
1	0.34	0.26	0.46	0.59	0.32
2	0.34	0.46	0.56	0.32	0.51
3	0.55	0.34	0.33	0.55	0.30
4	0.53	0.49	0.37	0.22	0.52
5	0.42	0.38	0.29	0.57	0.27
6	0.40	0.52	0.46	0.54	0.21
7	0.22	0.21	0.40	0.46	0.49
8	0.53	0.31	0.59	0.54	0.33
9	0.46	0.46	0.58	0.40	0.28

Statistical uncertainty: 2.5 MeV

LHC $\sqrt{s} = 13$ TeV, $M_{\ell\ell} = M_Z$, $y_{\ell\ell} = 0$



TMD factorisation

- 🍎 TMD factorisation introduces two independent scales:
 - 🍎 the **renormalisation scale μ** , originating from the UV renormalisation,
 - 🍎 the **rapidity scale ζ** , originating from the cancellation of rapidity divergences.

- 🍎 The respective **evolution equations** are:

$$\frac{\partial \ln F}{\partial \ln \sqrt{\zeta}} = K(\mu_0) - \int_{\mu_0}^{\mu} \frac{d\mu'}{\mu'} \gamma_K(\alpha_s(\mu'))$$

$$\frac{\partial \ln F}{\partial \ln \mu} = \gamma_F(\alpha_s(\mu)) - \gamma_K(\alpha_s(\mu)) \ln \frac{\sqrt{\zeta}}{\mu}$$

- 🍎 At small b_T , TMDs can be matched onto collinear distributions:

$$F(\mu, \zeta) = C(\mu, \zeta) \otimes f(\mu)$$

- 🍎 The solution final is:

$$\mu_b = b_0 / b_T$$

$$F(\mu, \zeta) = \exp \left\{ K(\mu_0) \ln \frac{\sqrt{\zeta}}{\sqrt{\zeta_0}} + \int_{\mu_0}^{\mu} \frac{d\mu'}{\mu'} \left[\gamma_F(\alpha_s(\mu')) - \gamma_K(\alpha_s(\mu')) \ln \frac{\sqrt{\zeta}}{\mu'} \right] \right\} C(\mu_0, \zeta_0) \otimes f(\mu_0)$$

- 🍎 Anomalous dims. and matching funcs. **perturbatively** computable. 38

TMD factorisation

Final expression:

$$F_{f/P}(x, \mathbf{b}_T; \mu, \zeta) = \sum_j C_{f/j}(x, b_*; \mu_b, \mu_b^2) \otimes f_{j/P}(x, \mu_b)$$

: A

$$\times \exp \left\{ K(b_*; \mu_b) \ln \frac{\sqrt{\zeta}}{\mu_b} + \int_{\mu_b}^{\mu} \frac{d\mu'}{\mu'} \left[\gamma_F - \gamma_K \ln \frac{\sqrt{\zeta}}{\mu'} \right] \right\}$$

: B

$$\times \exp \left\{ g_{j/P}(x, b_T) + g_K(b_T) \ln \frac{\sqrt{\zeta_F}}{\sqrt{\zeta_{F,0}}} \right\}$$

: C

- matching onto the collinear region at $b_T \ll 1/\Lambda_{\text{QCD}}$,
- factorises as *hard* (perturbative) and *longitudinal* (*i.e.* collinear, non-perturbative).

- avoid the Landau pole,
- f_{NP} accounts for the introduction of b_* ,
- f_{NP} is non-perturbative thus **fit** to data.

- CS and RGE evolution,
- evolution in μ and ζ ,
- perturbative.

Logarithmic counting

$$\left(\frac{d\sigma}{dq_T} \right)_{\text{res.}} \stackrel{\text{TMD}}{=} \sigma_0 \textcolor{violet}{H}(Q) \int d^2 \mathbf{b}_T e^{i \mathbf{b}_T \cdot \mathbf{q}_T} F_1(x_1, \mathbf{b}_T, Q, Q^2) F_2(x_2, \mathbf{b}_T, Q, Q^2)$$

$$F_i = \sum_j (\textcolor{brown}{C}_{i/j} \otimes f_j) \exp \left\{ \textcolor{green}{K} \ln \frac{\sqrt{\zeta}}{\mu_b} + \int_{\mu_b}^{\mu} \frac{d\mu'}{\mu'} \left[\textcolor{blue}{\gamma_F} - \textcolor{red}{\gamma_K} \ln \frac{\sqrt{\zeta}}{\mu'} \right] \right\}$$

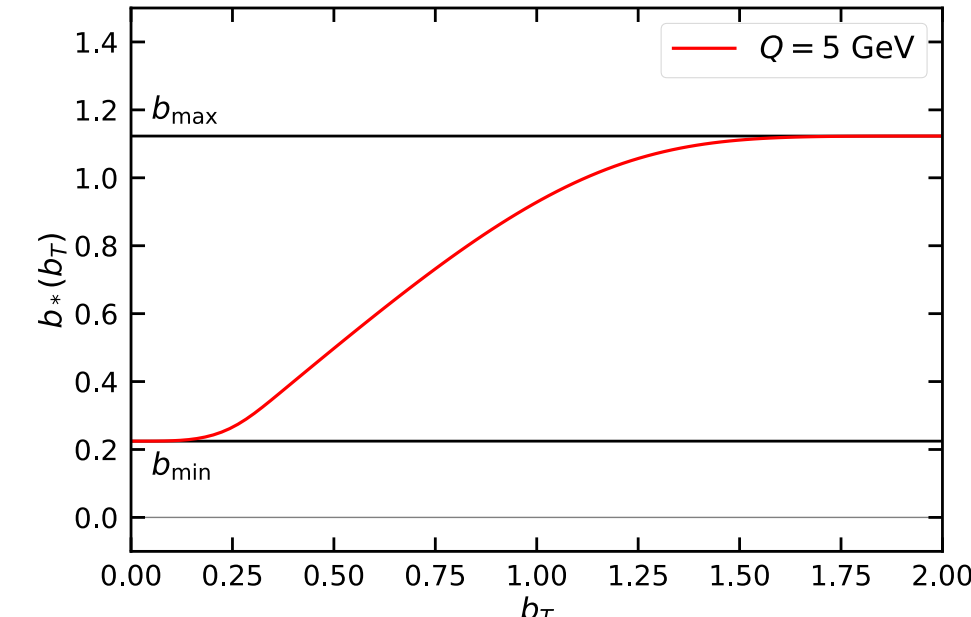
Accuracy	γ_K	γ_F	K	$C_{f/j}$	H	FFs/PDFs/ α_s
LL	α_s	-	-	1	1	-
NLL	α_s^2	α_s	α_s	1	1	LO
NLL'	α_s^2	α_s	α_s	α_s	α_s	LO
N^2LL	α_s^3	α_s^2	α_s^2	α_s	α_s	NLO
N^2LL'	α_s^3	α_s^2	α_s^2	α_s^2	α_s^2	NLO
N^3LL	α_s^4	α_s^3	α_s^3	α_s^2	α_s^2	NNLO
N^3LL'	α_s^4	α_s^3	α_s^3	α_s^3	α_s^3	NNLO

MAPTMD 2022

Main settings

- 🍎 b_* prescription:

$$b_*(b_T) = b_{\max} \left(\frac{1 - e^{-b_T^4/b_{\max}^4}}{1 - e^{-b_T^4/b_{\min}^4}} \right)^{1/4} \quad \text{with} \quad \begin{cases} b_{\max} = 2e^{-\gamma_E} \\ b_{\min} = b_{\max}/Q \end{cases}$$



- 🍎 Non-perturbative function f_{NP} :

🍎 evolution (CS kernel): $g_K(\mathbf{b}_T^2) = -g_2^2 \frac{\mathbf{b}_T^2}{2}$

- 🍎 PDFs:

$$f_{1NP}(x, \mathbf{b}_T^2; \zeta, Q_0) = \frac{g_1(x) e^{-g_1(x) \frac{\mathbf{b}_T^2}{4}} + \lambda^2 g_{1B}^2(x) \left[1 - g_{1B}(x) \frac{\mathbf{b}_T^2}{4} \right] e^{-g_{1B}(x) \frac{\mathbf{b}_T^2}{4}} + \lambda_2^2 g_{1C}(x) e^{-g_{1C}(x) \frac{\mathbf{b}_T^2}{4}}}{g_1(x) + \lambda^2 g_{1B}^2(x) + \lambda_2^2 g_{1C}(x)} \left[\frac{\zeta}{Q_0^2} \right]^{g_K(\mathbf{b}_T^2)/2}$$

- 🍎 FFs:

$$D_{1NP}(z, \mathbf{b}_T^2; \zeta, Q_0) = \frac{g_3(z) e^{-g_3(z) \frac{\mathbf{b}_T^2}{4z^2}} + \frac{\lambda_F}{z^2} g_{3B}^2(z) \left[1 - g_{3B}(z) \frac{\mathbf{b}_T^2}{4z^2} \right] e^{-g_{3B}(z) \frac{\mathbf{b}_T^2}{4z^2}}}{g_3(z) + \frac{\lambda_F}{z^2} g_{3B}^2(z)} \left[\frac{\zeta}{Q_0^2} \right]^{g_K(\mathbf{b}_T^2)/2}$$

$$g_{\{1,1B,1C\}}(x) = N_{\{1,1B,1C\}} \frac{x^{\sigma_{\{1,2,3\}}} (1-x)^{\alpha_{\{1,2,3\}}^2}}{\hat{x}^{\sigma_{\{1,2,3\}}} (1-\hat{x})^{\alpha_{\{1,2,3\}}^2}} \quad g_{\{3,3B\}}(z) = N_{\{3,3B\}} \frac{(z^{\beta_{\{1,2\}}} + \delta_{\{1,2\}}^2)(1-z)^{\gamma_{\{1,2\}}^2}}{(\hat{z}^{\beta_{\{1,2\}}} + \delta_{\{1,2\}}^2)(1-\hat{z})^{\gamma_{\{1,2\}}^2}}$$

- 🍎 11 (PDFs) + 9 (FFs) + 1 (evol): **21 free parameters** to fit to data.
- 🍎 Perturbative accuracies: **N³LL(-)**.
- 🍎 **Monte Carlo** method for the experimental error propagation.

MAPTMD 2022

Dataset



DY data:

- 🍎 fixed-target low-energy DY,
- 🍎 RHIC data,
- 🍎 LHC and Tevatron data,
- 🍎 selection cut $q_T / Q < 0.2$,
- 🍎 484 data points.



SIDIS data:

- 🍎 HERMES and COMPASS,
- 🍎 $P_{hT}|_{\max} = \min[\min[0.2Q, 0.5zQ] + 0.3 \text{ GeV}, zQ]$

🍎 $Q > 1.4 \text{ GeV}$, $0.2 < z < 0.7$,

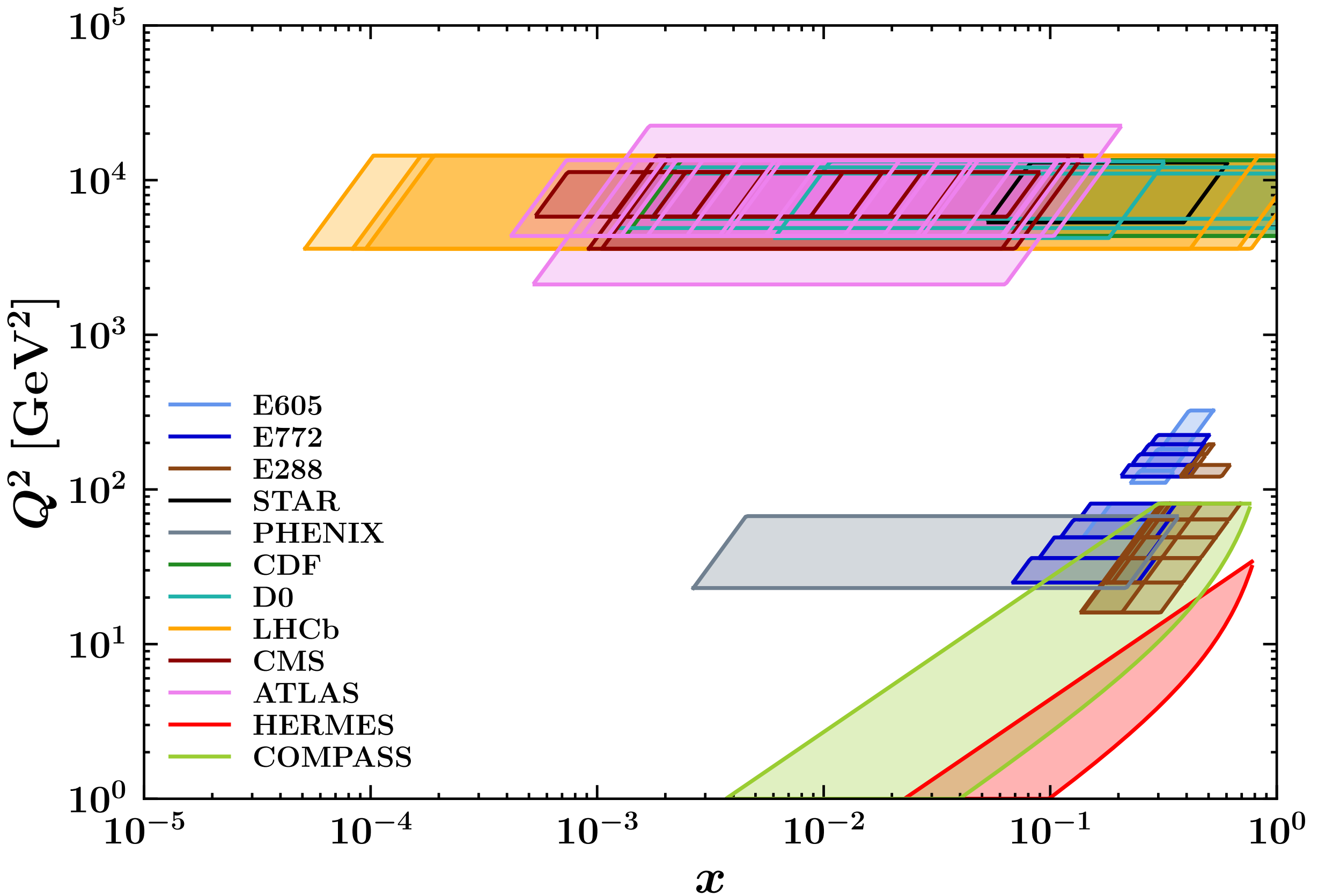
🍎 1547 points.

Experiment	N_{dat}	Observable	$\sqrt{s} [\text{GeV}]$	$Q [\text{GeV}]$	y or x_F	Lepton cuts	Ref.
E605	50	$Ed^3\sigma/d^3q$	38.8	7 - 18	$x_F = 0.1$	-	[55]
E772	53	$Ed^3\sigma/d^3q$	38.8	5 - 15	$0.1 < x_F < 0.3$	-	[51]
E288 200 GeV	30	$Ed^3\sigma/d^3q$	19.4	4 - 9	$y = 0.40$	-	[56]
E288 300 GeV	39	$Ed^3\sigma/d^3q$	23.8	4 - 12	$y = 0.21$	-	[56]
E288 400 GeV	61	$Ed^3\sigma/d^3q$	27.4	5 - 14	$y = 0.03$	-	[56]
STAR 510	7	$d\sigma/d q_T $	510	73 - 114	$ y < 1$	$p_{T\ell} > 25 \text{ GeV}$ $ \eta_\ell < 1$	-
PHENIX200	2	$d\sigma/d q_T $	200	4.8 - 8.2	$1.2 < y < 2.2$	-	[52]
CDF Run I	25	$d\sigma/d q_T $	1800	66 - 116	Inclusive	-	[57]
CDF Run II	26	$d\sigma/d q_T $	1960	66 - 116	Inclusive	-	[58]
D0 Run I	12	$d\sigma/d q_T $	1800	75 - 105	Inclusive	-	[59]
D0 Run II	5	$(1/\sigma)d\sigma/d q_T $	1960	70 - 110	Inclusive	-	[60]
D0 Run II (μ)	3	$(1/\sigma)d\sigma/d q_T $	1960	65 - 115	$ y < 1.7$	$p_{T\ell} > 15 \text{ GeV}$ $ \eta_\ell < 1.7$	[61]
LHCb 7 TeV	7	$d\sigma/d q_T $	7000	60 - 120	$2 < y < 4.5$	$p_{T\ell} > 20 \text{ GeV}$ $2 < \eta_\ell < 4.5$	[62]
LHCb 8 TeV	7	$d\sigma/d q_T $	8000	60 - 120	$2 < y < 4.5$	$p_{T\ell} > 20 \text{ GeV}$ $2 < \eta_\ell < 4.5$	[63]
LHCb 13 TeV	7	$d\sigma/d q_T $	13000	60 - 120	$2 < y < 4.5$	$p_{T\ell} > 20 \text{ GeV}$ $2 < \eta_\ell < 4.5$	[64]
CMS 7 TeV	4	$(1/\sigma)d\sigma/d q_T $	7000	60 - 120	$ y < 2.1$	$p_{T\ell} > 20 \text{ GeV}$ $ \eta_\ell < 2.1$	[65]
CMS 8 TeV	4	$(1/\sigma)d\sigma/d q_T $	8000	60 - 120	$ y < 2.1$	$p_{T\ell} > 15 \text{ GeV}$ $ \eta_\ell < 2.1$	[66]
CMS 13 TeV	70	$d\sigma/d q_T $	13000	76 - 106	$ y < 0.4$ $0.4 < y < 0.8$ $0.8 < y < 1.2$ $1.2 < y < 1.6$ $1.6 < y < 2.4$	$p_{T\ell} > 25 \text{ GeV}$ $ \eta_\ell < 2.4$	[53]
ATLAS 7 TeV	6 6 6	$(1/\sigma)d\sigma/d q_T $	7000	66 - 116	$ y < 1$ $1 < y < 2$ $2 < y < 2.4$	$p_{T\ell} > 20 \text{ GeV}$ $ \eta_\ell < 2.4$	[67]
ATLAS 8 TeV on-peak	6 6 6 6 6	$(1/\sigma)d\sigma/d q_T $	8000	66 - 116	$ y < 0.4$ $0.4 < y < 0.8$ $0.8 < y < 1.2$ $1.2 < y < 1.6$ $1.6 < y < 2$ $2 < y < 2.4$	$p_{T\ell} > 20 \text{ GeV}$ $ \eta_\ell < 2.4$	[68]
ATLAS 8 TeV off-peak	4 8	$(1/\sigma)d\sigma/d q_T $	8000	46 - 66 116 - 150	$ y < 2.4$	$p_{T\ell} > 20 \text{ GeV}$ $ \eta_\ell < 2.4$	[68]
ATLAS 13 TeV	6	$(1/\sigma)d\sigma/d q_T $	13000	66 - 113	$ y < 2.5$	$p_{T\ell} > 27 \text{ GeV}$ $ \eta_\ell < 2.5$	[54]
Total	484						

Experiment	N_{dat}	Observable	Channels	$Q [\text{GeV}]$	x	z	Phase space cuts	Ref.
HERMES	344	$M(x, z, \mathbf{P}_{hT} , Q)$	$p \rightarrow \pi^+$ $p \rightarrow \pi^-$ $p \rightarrow K^+$ $p \rightarrow K^-$ $d \rightarrow \pi^+$ $d \rightarrow \pi^-$ $d \rightarrow K^+$ $d \rightarrow K^-$	$1 - \sqrt{15}$	$0.023 < x < 0.6$ (6 bins)	$0.1 < z < 1.1$ (8 bins)	$W^2 > 10 \text{ GeV}^2$ $0.1 < y < 0.85$	[46]
COMPASS	1203	$M(x, z, \mathbf{P}_{hT}^2, Q)$	$d \rightarrow h^+$ $d \rightarrow h^-$	$1 - 9$ (5 bins)	$0.003 < x < 0.4$ (8 bins)	$0.2 < z < 0.8$ (4 bins)	$W^2 > 25 \text{ GeV}^2$ $0.1 < y < 0.9$	[72]
Total	1547							

MAPTMD 2022

Kinematic coverage



MAPTMD 2022

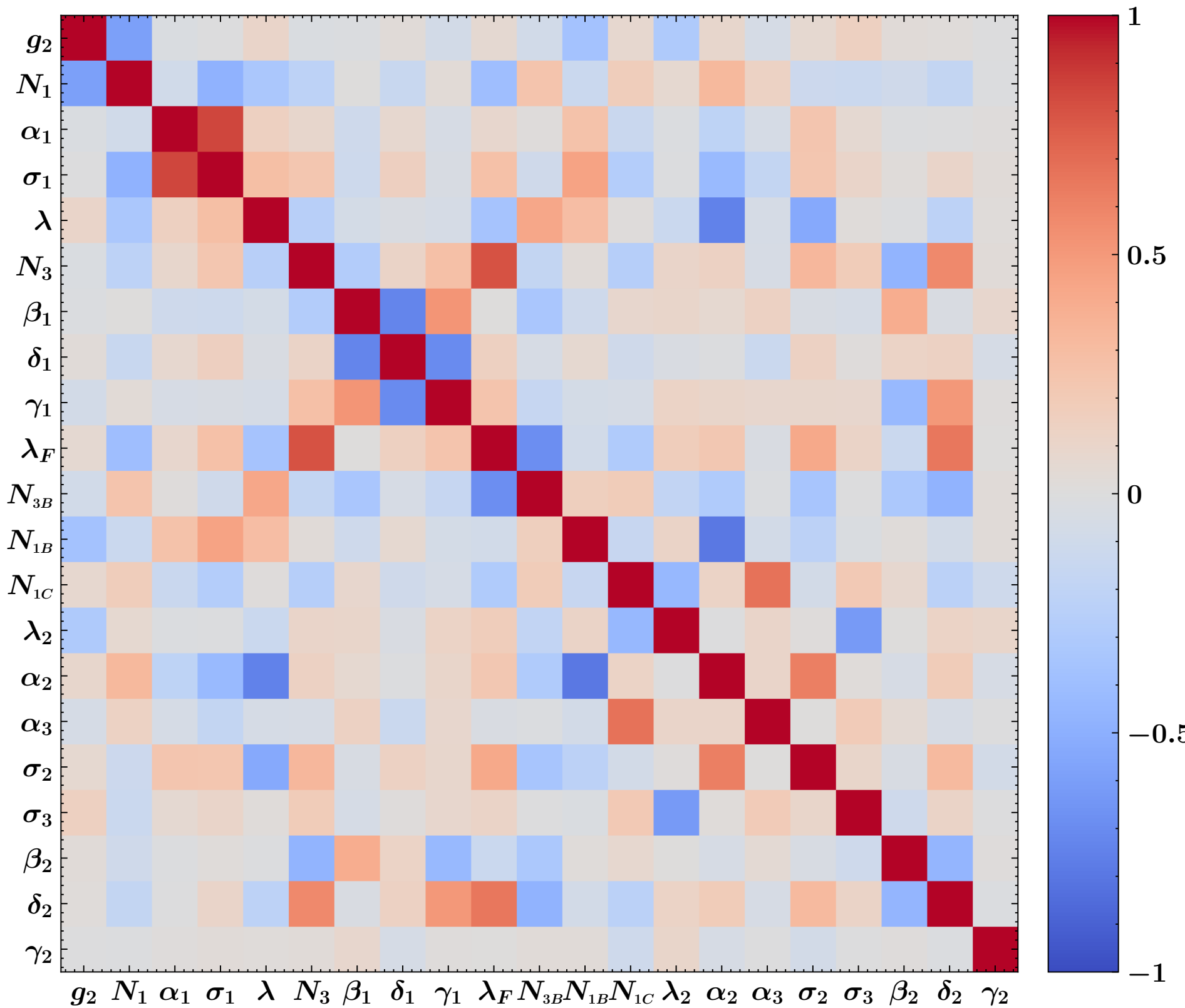
Fit quality

Data set	N ³ LL−			
	N_{dat}	χ^2_D	χ^2_λ	χ^2_0
CDF Run I	25	0.45	0.09	0.54
CDF Run II	26	0.995	0.004	1.0
D0 Run I	12	0.67	0.01	0.68
D0 Run II	5	0.89	0.21	1.10
D0 Run II (μ)	3	3.96	0.28	4.2
<i>Tevatron total</i>	71	0.87	0.06	0.93
LHCb 7 TeV	7	1.24	0.49	1.73
LHCb 8 TeV	7	0.78	0.36	1.14
LHCb 13 TeV	7	1.42	0.06	1.48
<i>LHCb total</i>	21	1.15	0.3	1.45
ATLAS 7 TeV	18	6.43	0.92	7.35
ATLAS 8 TeV	48	3.7	0.32	4.02
ATLAS 13 TeV	6	5.9	0.5	6.4
<i>ATLAS total</i>	72	4.56	0.48	5.05
CMS 7 TeV	4	2.21	0.10	2.31
CMS 8 TeV	4	1.938	0.001	1.94
CMS 13 TeV	70	0.36	0.02	0.37
<i>CMS total</i>	78	0.53	0.02	0.55
PHENIX 200	2	2.21	0.88	3.08
STAR 510	7	1.05	0.10	1.15
DY collider total	251	1.86	0.2	2.06

E288 200 GeV	30	0.35	0.19	0.54
E288 300 GeV	39	0.33	0.09	0.42
E288 400 GeV	61	0.5	0.11	0.61
E772	53	1.52	1.03	2.56
E605	50	1.26	0.44	1.7
DY fixed-target total	233	0.85	0.4	1.24
HERMES ($p \rightarrow \pi^+$)	45	0.86	0.42	1.28
HERMES ($p \rightarrow \pi^-$)	45	0.61	0.31	0.92
HERMES ($p \rightarrow K^+$)	45	0.49	0.04	0.53
HERMES ($p \rightarrow K^-$)	37	0.18	0.13	0.31
HERMES ($d \rightarrow \pi^+$)	41	0.68	0.45	1.13
HERMES ($d \rightarrow \pi^-$)	45	0.63	0.35	0.97
HERMES ($d \rightarrow K^+$)	45	0.2	0.02	0.22
HERMES ($d \rightarrow K^-$)	41	0.14	0.08	0.22
<i>HERMES total</i>	344	0.48	0.23	0.71
COMPASS ($d \rightarrow h^+$)	602	0.55	0.31	0.86
COMPASS ($d \rightarrow h^-$)	601	0.68	0.3	0.98
<i>COMPASS total</i>	1203	0.62	0.3	0.92
SIDIS total	1547	0.59	0.28	0.87
Total	2031	0.77	0.29	1.06

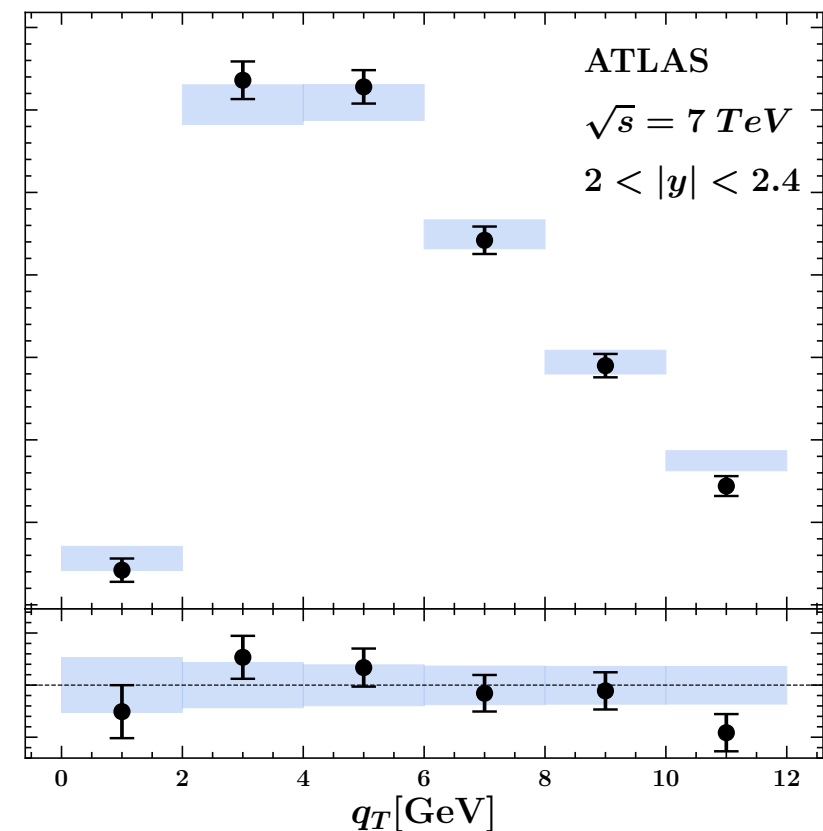
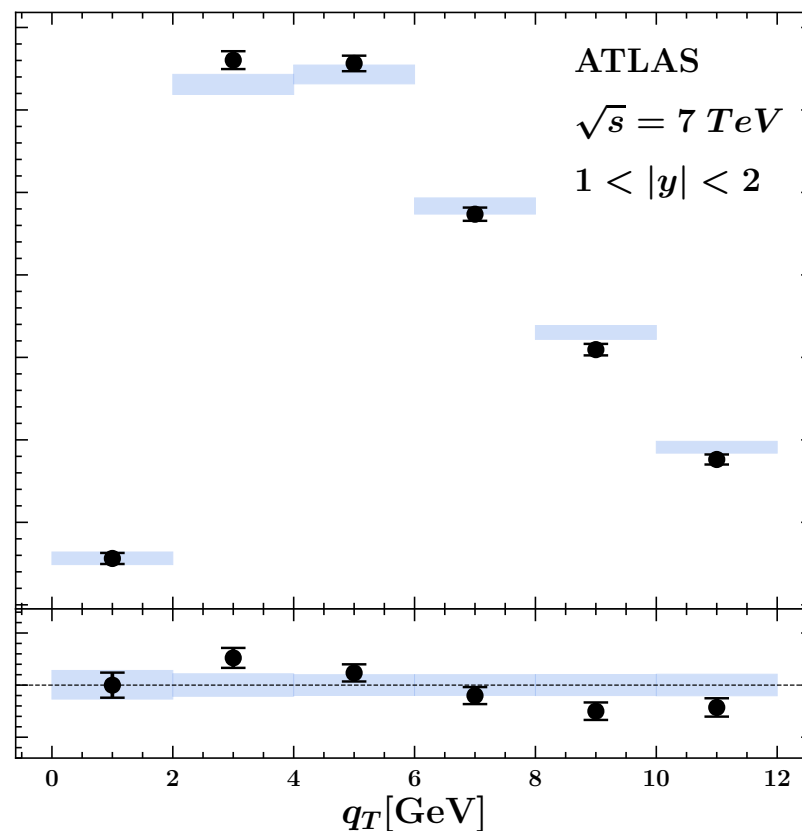
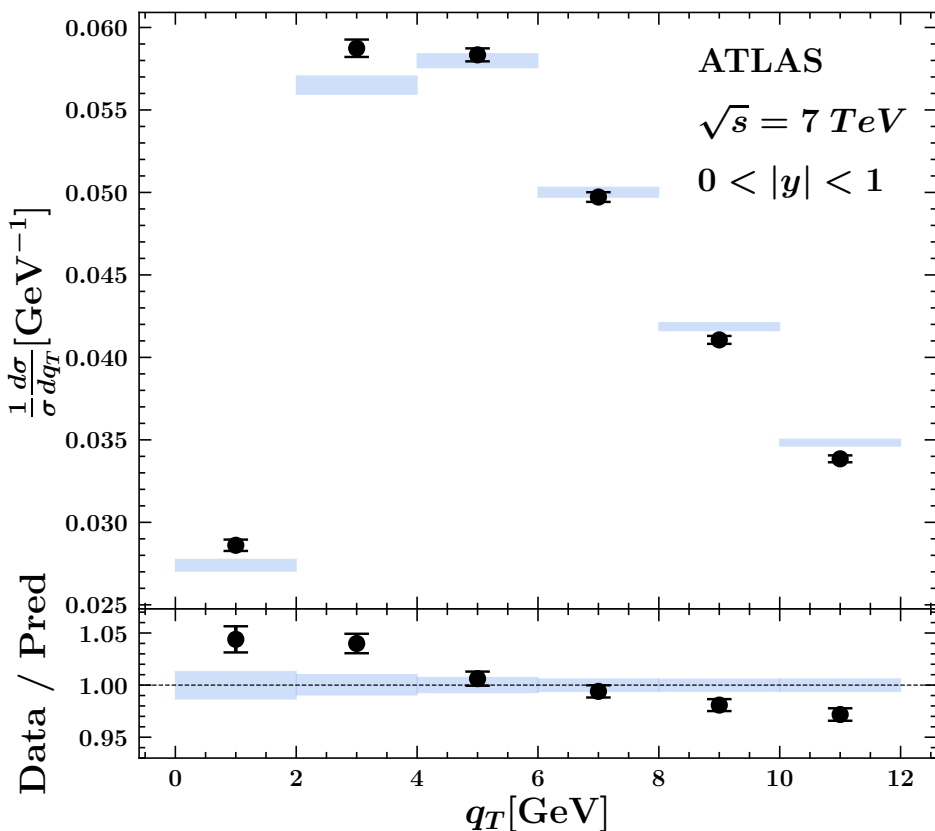
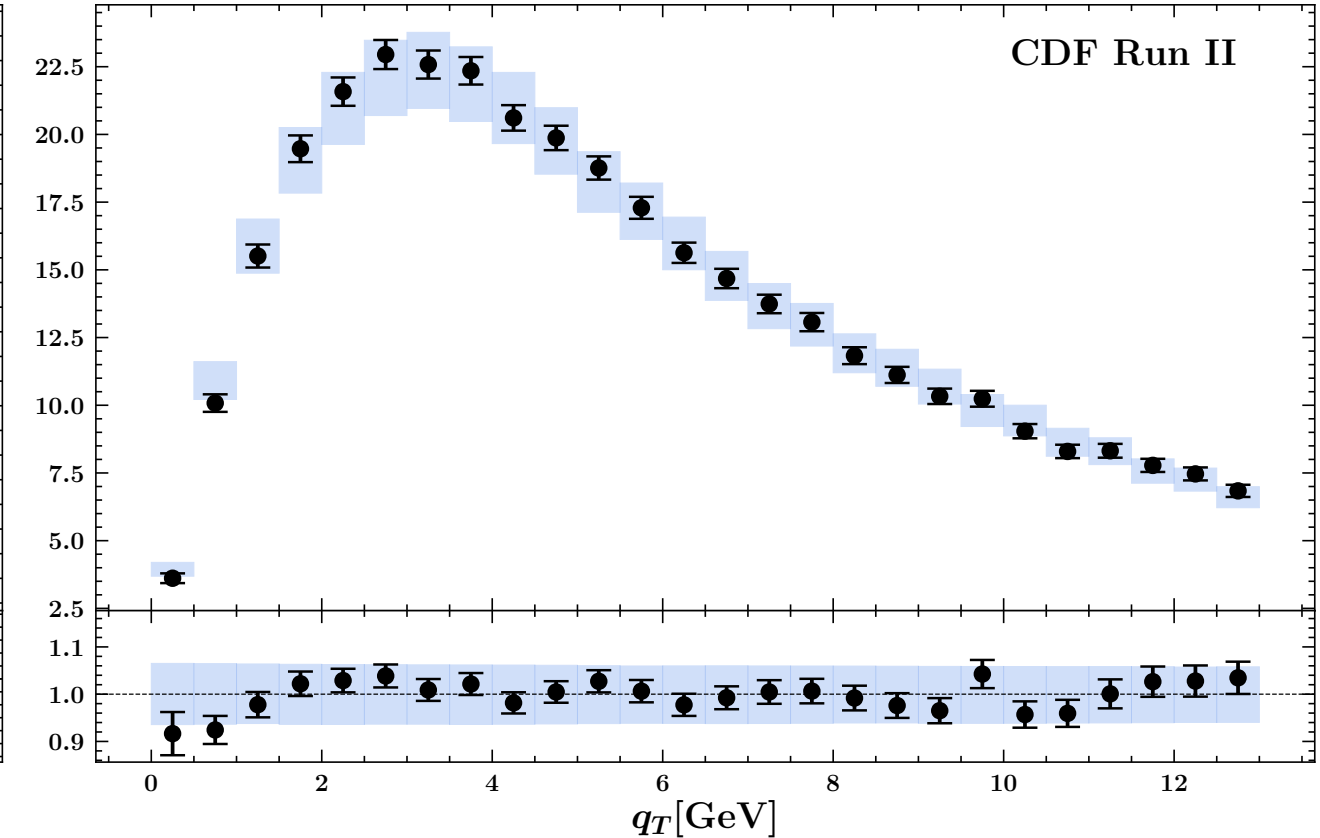
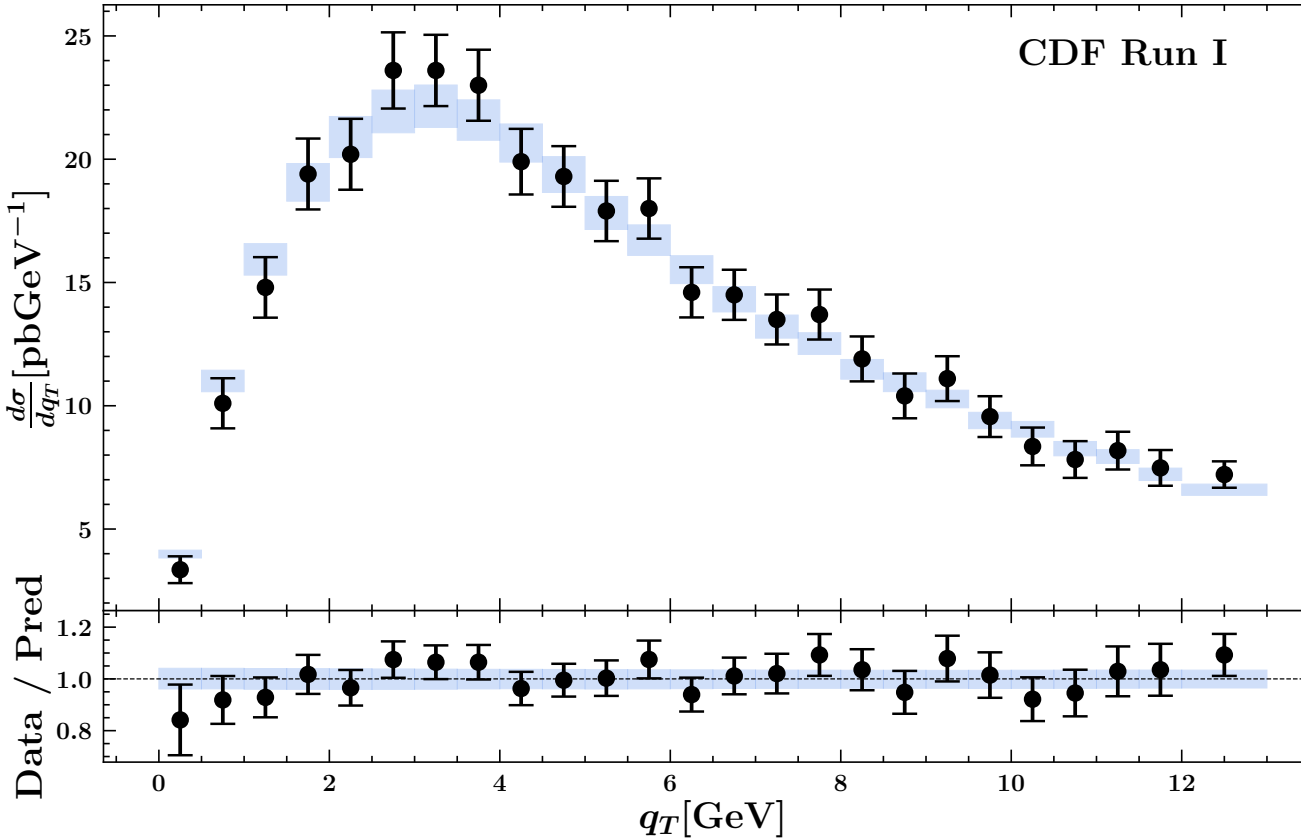
MAPTMD 2022

Correlation between fit parameters



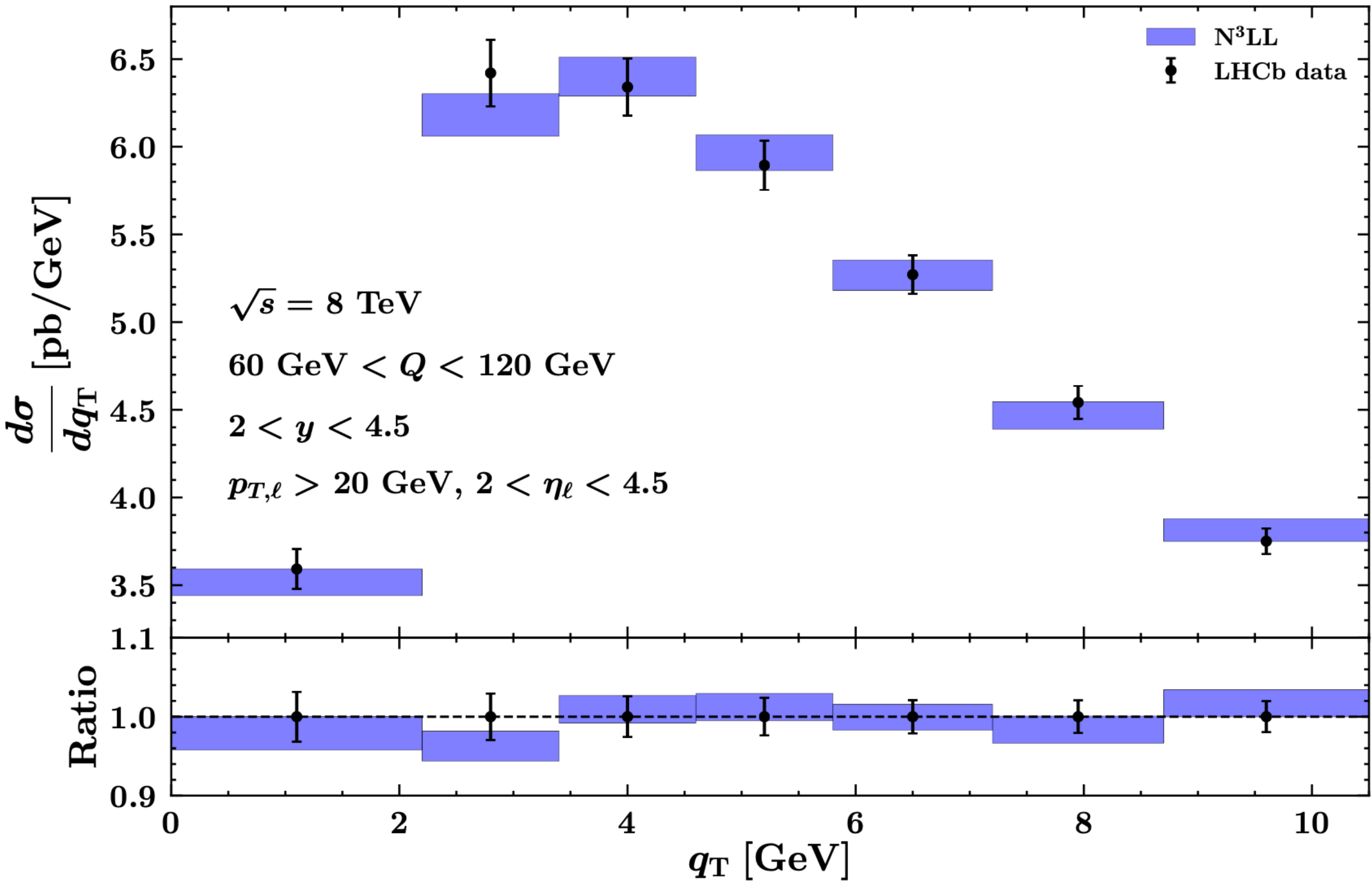
MAPTMD 2022

Fit quality: DY



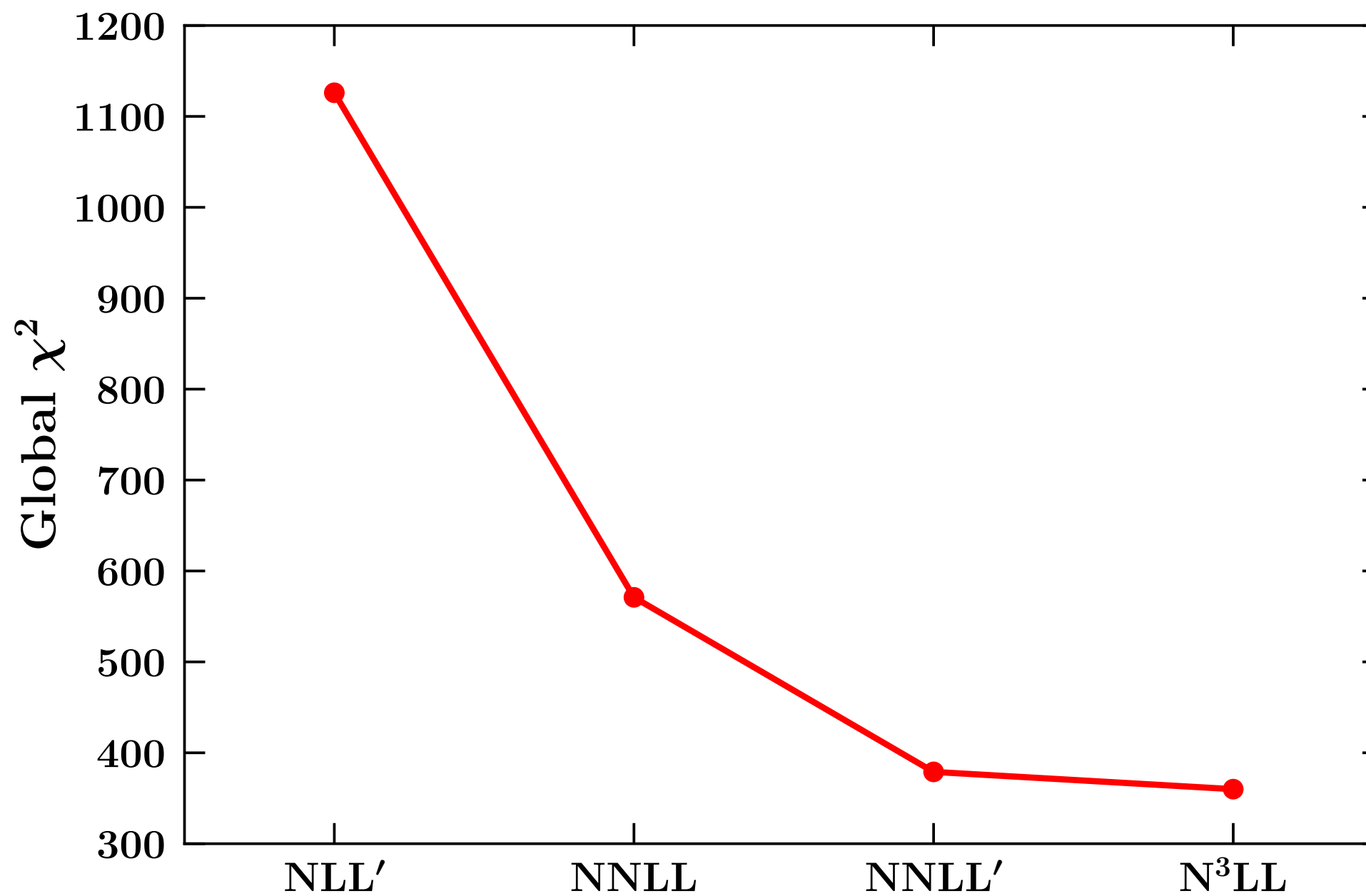
MAPTMD 2022

Fit quality: DY at LHCb



Perturbative convergence

	NLL'	NNLL	NNLL'	N^3LL
Global χ^2	1126	571	379	360



Perturbative convergence

